CHAPTER 5

ACETONE + CARBON DIOXIDE MIXTURES AT HIGH PRESSURES

The binary fluid mixtures of carbon dioxide with organic solvents at high pressures are widely used in extractions and separations, chemical reactions, and material processing (Kiran and Sengers, 1994; McHugh and Krukonis, 1994; Brunner, 2004; Reverchon et. al., 2003; Tomasko et. al., 2003a; b). Depending upon the composition, these mixtures are often carbon dioxide modified with an organic "cosolvent" or are organic solvents modified (expanded) with carbon dioxide. Even though processing with carbon dioxide at low levels of organic solvent additives as cosolvents is of continuing interest, in recent years there has been a growing activity in using carbon dioxide expanded liquids (Anand et. al., 2005; Shukla et. al., 2006). The terminology of expanded liquids is used without always clear documentation if indeed the mixtures show positive excess volumes. In our laboratory, we are interested in organic solvents modified with carbon dioxide such as alkane + carbon dioxide, THF + carbon dioxide, and more recently acetone + carbon dioxide as tunable solvents for polymerizations and polymer modifications. We have investigated the volumetric properties of a series of organic solvent + carbon dioxide mixtures in the past. (Pöhler and Kiran, 1997a; b; c) We now present new data on the density, viscosity, and excess volume of acetone + carbon dioxide mixtures.

A number of studies have already appeared on mixtures of acetone + carbon dioxide. Reaves and coworkers (Reaves et. al., 1998) measured the critical points for acetone + carbon dioxide mixtures for acetone compositions up to 7.0 mol %. Day (Day et. al., 1996) and Chang (Chang et. al., 1997) reported phase equilibria in acetone + carbon dioxide mixtures at temperatures in the range 291 – 313 K at pressures up to 8 MPa. Additional data at 323 and 333 K have been recently reported (Adrian and Maurer, 1997; Bamberger and Maurer, 2000; Stievano and Elavassore, 2005). The liquid-vapor phase boundaries of these mixtures at high pressures were determined by Chen (Chen et. al., 2003) and Wu (Wu et. al., 2005). The densities and excess volumes were reported by Pöhler and Kiran (Pöhler and Kiran, 1997a), and Wu (Wu et. al., 2004). Some transport properties of the mixture such as diffusion coefficient of acetone in carbon dioxide were also reported (Umezawa and Nagashima, 1992; Funazukuri et. al., 2000). Even though phase equilibria have been studied, the high-pressure viscosity data for this mixture is limited. To our knowledge, only Tilly and coworkers (Tilly et. al., 1994) reported viscosity for this mixture for acetone concentrations between 1 to 5 mol % at 313 and 323 K and at pressures up to 24 MPa. We have recently reported viscosity data for acetone, and for solutions of poly (methyl methacrylate) and poly (ε-caprolactone) in acetone, or in acetone + carbon dioxide mixtures (Liu et. al., 2006; Liu and Kiran, 2006).

We now report on the density and viscosity for acetone, carbon dioxide, and acetone + carbon dioxide mixtures containing 10, 25, 50, and 75 wt % carbon dioxide at 323, 348, 373, and 398 K and at pressures up to 35 MPa. The flow activation volumes and flow activation energies that are derived from the variation of viscosity with pressure and temperature are also reported. Free volume-based density correlations and close - packed volumes obtained

from such correlations are also presented. For the mixtures, we report the excess volume over the full composition range. We also present a comparative assessment of several mixing rules for predicting the viscosities of these mixtures.

5.1 Experimental procedures

A high-pressure-high-temperature falling-cylinder type viscometer, shown in Figure 4.6 in Chapter 4 and described in Chapter 4 as well, was used to determine the viscosity and density of the mixtures simultaneously. The pressure is adjusted at any loading and temperature, by changing the position of a movable piston (PI). The position of the piston (and thus the internal volume) is recorded at any given temperature and pressure. Knowing the internal volume permits the determination of the density at a given T and P since initial mass loading is known. The fall of the sinker is initiated by demagnetization of the pull-up magnet (PM). The fall time of the sinker is monitored by three linear-variable differential transformer units (LVDT I, II and III) positioned along the fall-tube. The signal from each LVDT (as voltage reading) is recorded as a function of time when the sinker falls through the full length of the fall tube and is further processed to generate distance versus fall time plots for the sinker from which the terminal velocity (V_t) is determined. The terminal velocity along with density is then used to determine viscosity using the following equation

$$\eta = \frac{1}{V_t}(\rho_s - \rho_f)K \qquad \text{(Eq.5.1)}$$

where ρ_s is the density of the sinker, ρ_f is the density of the fluid, V_t is the terminal velocity of the sinker, K is a calibration constant, which is determined by measuring the terminal velocity and density of systems of known viscosities. With this instrument, the

system temperature and pressure are measured with an accuracy of ± 0.1 K and ± 0.06 MPa, respectively. Densities and viscosities are measured with an accuracy of 1.5 and 4 %, respectively (Liu and Kiran, 2006). Acetone (Burdick & Jackson) with purity of 99.5 % and CO_2 (Airgas) with a minimum purity of 99.9 % were used without further purification.

5.2 Results and discussion

Table 5.1 summarizes the viscosity and density data for pure acetone, carbon dioxide and their mixtures determined at the nominal temperatures of 323, 348, 373, and 398 K at pressures up to 35 MPa. For the mixtures, the table also includes excess volume, excess viscosity, excess Gibbs free energy of viscous flow, and Grunberg-Nissan interaction parameter, which will be discussed later. The present measurements were mostly carried out at pressures greater than 12 MPa, which are higher than the critical pressures reported for these mixtures (Pöhler and Kiran, 1997a). The mixtures are either supercritical or exist as liquid mixtures at most of the measurement conditions.

5.2.1 Density

Figure 5.1 displays the variation of density with pressure for each mixture at the nominal temperature of 323 K. The density data for pure acetone and pure carbon dioxide which is generated using a variable-volume view cell from an earlier study (Pöhler and Kiran, 1997a) conducted in our laboratory and are included for comparisons. The data for the acetone + carbon dioxide mixtures containing about 50 wt % carbon dioxide (Chen et. al., 2003) are also included. Although slight differences in the densities are observed, the agreements

between the experimental data and the literature data are still good. Density increases with pressure for all mixtures, but $\partial\rho/\partial P$ for carbon dioxide is much larger than that for the mixtures -- leading to a density crossover around 18 MPa for mixtures containing less than 50 wt % carbon dioxide, and around 23 MPa for mixtures with greater than 50 wt % CO_2. Density crossover is a well-known behavior in mixtures of CO_2 with organic solvents (Pöhler and Kiran, 1997a, b, c). Figure 5.2 shows the density variation with pressure at a higher temperature, T = 348 K. The density crossover pressures are observed to increase to around 30 MPa (for CO_2 content less than 50 wt %) and 35 MPa (for CO_2 content higher than 50 wt %). Figure 5.3 displays the variation of density with temperature for the mixture containing 10 wt % carbon dioxide at 7, 14, 21, 28, and 35 MPa. The densities show essentially linear decrease with temperature at all the pressures.

5.2.2 Viscosity

Figure 5.4 shows the variation of viscosity with pressure for pure acetone, carbon dioxide and their mixtures at the nominal temperature of 323 K. The literature viscosity data (Stephan and Lucas, 1978) for carbon dioxide are also included in the figure for comparisons. The insert is an enlargement of the carbon dioxide data. Mixtures all show viscosities lower than that of acetone and the viscosity reduction increases with the carbon dioxide content. A 60 % reduction in viscosity is observed for the mixture containing 50 wt % carbon dioxide. Figure 5.5 illustrates the variation of viscosity with temperature for mixtures containing 10 wt % carbon dioxide at 7, 14, 21, 28, and 35 MPa. The viscosities were found to shown linear decease with temperature in the range studied.

5.2.3 Flow activation volume and flow activation energy

We have analyzed the variation of viscosity with pressure for all temperatures, and with temperature for all pressures given in Table 5.1 in a manner shown in Figures 5.4 and 5.5 and correlated the data using the relationships (Xiong and Kiran, 1995; Yeo and Kiran, 1999):

$$\eta = A\exp(V^{\neq}P/RT) \qquad \text{(Eq.5.2)}$$

and

$$\eta = B\exp\left(E^{\neq}/RT\right) \qquad \text{(Eq.5.3)}$$

where η is the viscosity, A and B are constants, $V^{\neq}$ and $E^{\neq}$ are the flow activation volume and flow activation energy, P is the pressure, R is the gas constant and T is the temperature. The parameters for these equations are given in Tables 5.2 and 5.3 along with the correlation coefficients and average absolute deviation (AAD) values. The flow activation energies were in the range of 5 – 10 kJ/mol, for most mixtures the value being around 8 kJ/mol and independent of pressure. The flow activation volumes range from 5 to 41 cm^3/mol. For all the systems, the activation volumes show an increase with temperature and at a given temperature $V^{\neq}$ appears to also increase with carbon dioxide content in the mixture.

5.2.4 Viscosity – density correlation and close-packed volume

Figure 5.6 shows the variation of viscosity with density for acetone, carbon dioxide, and acetone + carbon dioxide mixtures containing 10, 25, 50, and 75 wt % carbon dioxide. This figure clearly demonstrates the change (reduction) in viscosity in going from acetone to carbon dioxide for all temperatures and pressures. The data was correlated using a free volume-based equation (Xiong and Kiran, 1995; Yeo and Kiran, 1999)

$$\eta = C \cdot \exp\left(\frac{D}{1 - V_0 \cdot \rho}\right) \qquad \text{(Eq.5.4)}$$

where C and D are constants, ρ is the density and V_0 is the close-packed volume for the mixtures. The Hooke-Jeeves and quasi-Newton method with convergence criterion of 0.0001 were used to find the parameters. The close-packed volumes, constants C, D, correlation coefficients and AADs of the correlations are summarized in Table 5.4. The close-packed volumes decrease from 0.98 cm^3/g (for acetone) to 0.45 cm^3/g (for carbon dioxide). In an earlier study we reported a close-packed volume of 0.29 cm^3/g for CO_2 based on correlations that were obtained from data generated at higher temperatures in the range 380 – 420 K (Xiong and Kiran, 1995). In the present study the temperatures are much lower, the range being 320-370 K. It should also be noted that for CO_2, close-packed volume that is predicted with the van der Waals model is 0.44 cm^3/g, which are similar to the values obtained from the experimental data at the present temperature range. Figure 5.6 is very instructive in showing the extent to which the viscosity is reduced by addition of carbon dioxide if density were held constant, and to what extent the mixture must be compressed if same viscosity were to be maintained for a given mixture. It should be pointed out that the data for each fluid or fluid mixture in Figure 5.6 represent wide range of P/T conditions, and the model has its limitations. The correlations that are better descriptors of viscosity versus density may be generated at each temperature. However, in the present publication our aim has been to provide a correlation that can be applicable over a wider range of P and T conditions.

5.2.5 Excess volume

The excess volumes were calculated as

$$V^E = V^{mix} - \sum_{i=1}^{n} x_i V_i \qquad \text{(Eq.5.5)}$$

where V^E is the molar excess volume (cm^3/mol), V^{mix} is the mixture molar volume (cm^3/mol), x_i and V_i are mole fraction and molar volume for component *i*. The mixture molar volume V^{mix} and the component molar volume V_i are calculated from,

$$V^{mix} = M_{mix} / \rho_{mix} \qquad \text{(Eq.5.6)}$$

and

$$V_i = M_i / \rho_i \qquad \text{(Eq.5.7)}$$

where ρ_{mix} and ρ_i are densities of the mixture and the pure component *i*, which were determined experimentally. M_{mix} and M_i are the molecular weights for the mixture and the component *i*. The mixture molecular weight M_{mix} are calculated as

$$M_{mix} = \sum_{i=1}^{n} M_i \times x_i \qquad \text{(Eq.5.8)}$$

Figure 5.7 shows the variation of excess volume with carbon dioxide content at 323 K and 14, 21, 28, and 35 MPa. Since the experimental data for pure components and the mixtures were at slightly different temperature, data were extrapolated to the same temperature values before calculation of the excess quantities. The excess volumes from an earlier study (Pöhler and Kiran, 1997a) for limited compositions of this mixture that were obtained at higher pressures (35 and 55 MPa) are also included to accentuate the trends. The excess volumes are negative for all compositions at low pressures (14 and 21 MPa). With an increase in pressure, excess volume becomes positive for mixtures with high carbon dioxide contents. At 28 MPa, positive excess volume is displayed for the mixture with a carbon dioxide content of 75 %.

As the pressures are increased, positive excess volumes are observed for mixtures at lower CO_2 content. At 55 MPa, all compositions appear to display positive excess volumes. The negative excess volumes for these mixtures indicate that overall volume of the mixture deceases upon mixing compared to simple linear additions. The concept of "expanded liquids" is frequently reserved for two-phase systems at low carbon dioxide pressures. One should however exercise caution in that these systems may not necessary mean that the volume of the organic liquid is actually expanded. It may even be reduced. If excess volumes are negative, the favorable attribute of the "liquid" arises from a combination of compositional effects and a change in the overall mixture density, rather than always a change in the volume of the organic solvent. Figure 5.8 shows the variation of excess volume with carbon dioxide content at 373 K for 28 and 35 MPa. The excess volumes are negative at these high pressures. Comparisons with Figure 5.7 show that higher temperature may lead to more negative excess volumes.

5.2.6 Correlations for mixture viscosity

Four different mixing rules were evaluated for their predictive ability of the mixture viscosities, expressed by the following equations:

$$\eta_{mix} = \sum_{i=1}^{n} x_i \eta_i \qquad \text{(Eq.5.9)}$$

$$\ln \eta_{mix} = \sum_{i=1}^{n} x_i \ln \eta_i \qquad \text{(Eq.5.10)}$$

$$\eta_{mix} V_{mix} = \sum_{i=1}^{n} x_i \eta_i V_i \qquad \text{(Eq.5.11)}$$

$$\ln(\eta_{mix} V_{mix}) = \sum_{i=1}^{n} x_i \ln(\eta_i V_i) \qquad \text{(Eq.5.12)}$$

Here η_{mix} and η_i are the viscosity of the mixture and the component *i*. V_{mix} and V_i are molar volumes. The logarithmic viscosity given by equations 5.10 and 5.12 are known as the "Grunberg-Nissan" (Grunberg and Nissan, 1949) and "Katti-Chaudhri" mixing rules, respectively. Equations 5.11 and 5.12 involve the product "ηV", which is the kinematic viscosity. Figures 5.9 and 5.10 show the comparisons of the predictions with the experimental data at 28 MPa, at two different temperatures. (The prediction corresponding to each experimental data points are specifically shown in these figures, which should not be confused with actual experimental data.) At 323 K, the logarithmic mixing rules describe the viscosity well but at the higher temperature, the simple linear combinations are observed to give better results. For all the mixing rules, in the viscosity range from 0.04 to 0.38 mPa·s, the average absolute deviation (AAD) between the model and the experimental data, depending upon the model and the temperature, is calculated to be in the range from 0.005 to 0.04 mPa·s.

5.2.7 Excess viscosity

The excess viscosity ($\Delta\eta$), defined as viscosity deviation from the arithmetic average of the component viscosities, were calculated according to

$$\Delta\eta = \eta_{mix} - \sum_{i=1}^{n} x_i \eta_i \qquad \text{(Eq.5.13)}$$

These excess viscosities were evaluated for possible correlations with fluid composition and /or the excess volume. Figure 5.11 and 5.12 show the variation of excess viscosity with carbon dioxide content at 323 K and 373 K at different pressures. The magnitude and sign of

the excess viscosity depend on the fluid composition. The excess viscosity is positive and goes through a maximum for the mixture containing 25 % carbon dioxide at both temperatures. Excess viscosities are negative for other mixtures at 323 K but become positive at 373 K. Pressure appears to influence the mixtures with higher carbon dioxide content and becomes larger at 373 K. Excess viscosity becomes less positive with increasing pressure.

Analysis of the excess viscosity with excess volume showed no simple correlations. At 323 K, both the excess viscosities and excess volumes were negative, at 373 K, excess viscosities were positive while excess volumes remained negative. This is illustrated in Figure 5.13.

Even though one anticipates a more clear and direct correlation between excess viscosity and excess volume, the present data and limited literature on other systems indicate that this is often not the case. For example in a recent publication (Sathyanarayana et. al., 2007) on mixtures of N-methylacetamide with chloroethanes and chloroethenes no correlations could be established between the sign of the excess viscosity and the sign of excess volume either. This was rationalized by noting that the excess viscosity must depend not only on the intermolecular interactions, but also on the sizes and shapes of the component molecules. In order to elucidate the importance of interactions between unlike molecules, they evaluated the excess Gibbs free energy of viscous flow ($G_V^{\ E}$) and Grunberg-Nissan interaction parameters (d_{12}) using the equations,

$$G_V^{\ E} = RT[\ln \eta_{mix} V_{mix} - (x_1 \ln \eta_1 V_1 + x_2 \ln \eta_2 V_2)] \qquad \text{(Eq.5.14)}$$

and

$$d_{12} = (\ln \eta_{mix} - x_1 \ln \eta_1 - x_2 \ln \eta_2)/(x_1 x_2) \qquad \text{(Eq.5.15)}$$

We have carried out such an analysis with our data as well. The calculated values of G_V^E and d_{12} are summarized in Table 5.1. Literature indicates that positive G_V^E values arise from specific chemical interactions while negative values indicate the dominance of physical interactions (arising from induction forces, dispersion forces and so on) (Sathyanarayana et. al., 2007; Reed and Taylor, 1959). If d_{12} values are positive, the interactions between unlike molecules are strong, whereas they become weak with negative values (Sathyanarayana et. al., 2007; Reed and Taylor, 1959). Except for the mixture containing 10 % carbon dioxide at 325 K, essentially all values of G_V^E and d_{12} in the Table 5.1 are positive, which suggest strong interactions between acetone and carbon dioxide at the conditions investigated.

The specific interaction between the carbon atom in carbon dioxide with the carbonyl group in acetone has been predicted in *ab initio* simulations (Nelson and Borkman, 1998; Danten et. al., 2002) and confirmed also in spectroscopic experiments (Blatchford et. al., 2003; Cabaco et. al., 2005) in the literature. These studies conducted for 1:1 mixtures indicate formation of two types of electron donor-acceptor (EDA) complexes of carbon dioxide and acetone which are illustrated in Figure 5.14. The carbon atom in CO_2 is the electron acceptor center and the oxygen atom of the carbonyl group in acetone is the electron donor center. For carbon dioxide, literature indicates presence of pair-wise interactions leading to the formation of dimers (Kolafa et. al., 2001; Bukowski et. al., 1999; Fedchenia and Schröder, 1997; Tsuzuki et. al., 1998). The dimers are either in a slipped parallel geometry or in a T- shaped saddle geometry with a C – C separation of 3.6 $\mathring{A}$ or 4.2 $\mathring{A}$, respectively. These are also shown in Figure 5.14. A crossed geometry has also been indicated for carbon dioxide dimers (Kolafa

et. al., 2001). Carbon dioxide trimers have been predicted as well (Kolafa et. al., 2001). Of these, the slipped parallel arrangement is indicated to be favored (Bukowski et. al., 1999).

There has been no report on how these interactions in carbon dioxide + acetone mixtures change with pressure, temperature or fluid composition except a recent investigation where Raman spectral changes have been reported for carbon dioxide-acetone mixtures at 313 K at pressures from 0.5 to 9 MPa (Cabaco et. al., 2005). Even though the spectral band intensity representative of CO_2 –acetone complex increased up to 3 MPa (where the liquid phase molar content of CO_2 is reported to be 0.43), no significant change was observed with further increase in pressure (Cabaco et. al., 2005). Figure 5.15 is a simplified cartoon depicting mixtures with different carbon dioxide-to-acetone ratios and provides some insights to the effect of composition. For the 1:1 mixture, we assume that all carbon dioxide molecules associate with the acetone molecules forming complexes of either type I or II. For mixtures with high CO_2 content, a portion of carbon dioxide is tied with acetone forming the complex, and the remainder is assumed as existing as unassociated molecules or as dimers. For mixtures with high acetone concentration, a portion of acetone is tied with carbon dioxide forming the complex and remainder is free acetone. The formation of dimers in CO_2 and the nature of the association with acetone depicted in Figure 5.14 and 5.15 would suggest that mixtures with high carbon dioxide content would be more sensitive to pressure, whereas those with high acetone content would be more sensitive to temperature. This is indeed observed in Figures 5.11 and 5.12.

The data in Figures 5.7 and 5.8 with the negative excess volumes are consistent with strong interactions. At 323 K, association effects are more effective and lead to greater volume reduction at lower pressures. When pressure is increased, and both fluids become dense, the relative reduction in occupied volume in the mixture becomes less, reducing the relative impact of association. When temperature is increased, the more negative excess volumes observed at higher pressures suggest that the degree of association may be lessened at higher temperatures but is promoted at higher pressures that would help bring the components to their closer proximity.

Negative excess volume, other factors being the same, would imply an increase in the free volume in the mixture and thus lead to an expectation of a negative excess viscosity. In Figure 5.11, with an initial increase in the carbon dioxide content of the mixture, the formation of the acetone – CO_2 complex generates sufficient free volume and lead to negative excess viscosity. Since the mixture is dominated with acetone the net outcome overmasks any effect of the larger size and potentially higher viscosity of the acetone-CO_2 complex. With further increase in the carbon dioxide content in the mixture, the relative amount of the complex increases, and even though free volume is still leading to a negative excess viscosity, the size effect of the complex appears to set in, resulting in a positive excess viscosity for the mixtures containing 25 wt % carbon dioxide. At higher carbon dioxide content and as 1:1 molar mixture is approached, and more and more of the acetone molecules become tied in the acetone-carbon dioxide complex, the additional carbon dioxide molecules now appear to serve as diluent molecules leading to the negative excess viscosities. As the pure carbon dioxide end of the spectrum is approached, excess viscosity goes to zero.

A clear description of excess viscosity behavior at different temperatures and pressures is however difficult without additional information on how the complex formation is influenced by these factors and which form of the complex has higher viscosity. Figure 5.13 would suggest that at higher temperatures where excess viscosity is positive while excess volume is negative, the size and shape of the acetone-carbon dioxide complex must play a more significant role as compared to the free volume reduction. Free volume reduction appears to be a more dominating factor at lower temperatures leading to the observed negative excess viscosities.

Figures 5.16 and 5.17 show the variation of the actual viscosity of the mixtures with excess volume at 323 and 373 K for different mixtures at different pressures. Along the direction of the arrows, data points correspond to mixtures with 0, 10, 25, 50, 75, and 100 mass % carbon dioxide. For the pure components excess volume is zero. Even though no simple correlation could be identified for excess viscosity and excess volume, Figures 7.17 and 7.18 both show that, in the direction along the arrows at each pressure, the mixture viscosities always decrease with an increase in carbon dioxide content.

5.3 Further discussion. Recent advances on free volume theory for viscosity

The free-volume based theories assume that a fluid consists of hard spheres, and the total volume consists of occupied and free-volume contributions. The displacement of a molecule depends on the redistribution of free-volume which enlarges the vacant site for a molecule to

diffuse into. The free-volume is the difference between the volumes of the system minus the hard-sphere volume (occupied volume) of the molecules. This is also the basis of the Doolittle equation (Given by Eq.5.4) that we have already discussed. The relationship of equation 5.4 with free volume can be seen from the following expressions:

$$\eta \approx C\exp(\frac{D}{f_V}) = C\exp(D\frac{V}{V-V_0}) = C\exp(D\frac{1/\rho}{1/\rho - V_0}) = C\exp(\frac{D}{1-\rho V_0}) \quad \text{(Eq. 5.16)}$$

A recent model that is also based on the free-volume concepts expresses the dynamic viscosity as

$$\eta = \eta_0 + \Delta\eta \quad \text{(Eq.5.17)}$$

where $\Delta\eta$ is the change in going from a dilute gas to a dense fluid (Allal et. al., 2001). The dilute gas viscosity is given by

$$\eta_0 = \frac{40.785\sqrt{MT}}{v_c^{2/3}\Omega^*}F_C \quad \text{(Eq.5.18)}$$

where v_c is the critical volume as suggested in the literature (Allal et. al., 2001). Ω^* is the reduced collision integral given by

$$\Omega^* = \frac{1.16145}{T^{*0.14874}} + \frac{0.52487}{\exp(0.77320T^*)} + \frac{2.16178}{\exp(2.43787T^*)} - (6.435E-4)T^{*0.14874}\sin(18.0323T^{*-0.76830} - 7.27371) \quad \text{(Eq.5.19)}$$

where $T^* = \frac{1.2593T}{T_c}$

The factor F_c is given by

$$F_c = 1 - 0.2756\omega \text{ for a nonpolar gas} \quad \text{(Eq.5.20)}$$

$$F_c = 1 - 0.2756\omega + 131.3\mu/(v_c T_c)^{1/2} \quad \text{(Eq.5.21)}$$

where μ is the dipole moment, ω is acentric factor. For acetone, $\mu = 2.88 Debye$ and $\omega = 0.304$ (Lide, 1990; Fried, 2003).

A new relationship has been proposed, which is given below:

$$\eta = \eta_0 + \frac{\rho l\left(E_0 + \frac{PM}{\rho}\right)}{\sqrt{3RTM}} \exp\left[B\left(\frac{E_0 + \frac{PM}{\rho}}{RT}\right)^{3/2}\right] \qquad \text{(Eq.5.22)}$$

where η and ρ are the viscosity and density at temperature T and pressure P. M is the molecular weight and R is the gas constant. There are three adjustable parameters: l, E_0, and B in this model given by equation 5.22. l is a characteristic parameter related to molecular length for energy dissipation; E_0 is connected to the barrier or energy that a molecule must cross to diffuse, B is stated to be characteristic of the "free volume overlap". The changes in these parameters with temperature, pressure, or the actual system would then provide new insights. $\frac{PM}{\rho}$ is an energy term (PV) related to generation of vacant sites, and E_0 is an energy term representing the barrier that must be overcome. Thus, the total energy associated with movement is $E = E_0 + \frac{PM}{\rho}$. Allal and coworkers (Allal et. al., 2001) has shown that the free volume fraction can be expressed as $f_V = \left(\frac{RT}{E}\right)^{3/2}$. Then, in terms of free volume, equation 5.22 becomes

$$\eta - \eta_0 = \rho l \sqrt{\frac{RT}{3M}} f_V^{-2/3} \exp\left(\frac{B}{f_V}\right) \qquad \text{(Eq.5.23)}$$

which is identical in form with the Doolittle equation. However, this new theory attaches new physical interpretation opportunity to the parameters. For example, the front parameter C in the Doolittle equation (Eq.5.16) can now be related to the molecular length. And the total energy is divided into a combination of terms that include energy for vacancy generation, and energy to overcome a barrier for a molecular movement.

We have reanalyzed the present viscosity data for acetone using this new model by determining the three characteristic model parameters by fitting all the experimental viscosity and density data (generated at T = 323, 348, 373, and 398 K; P = 7, 14, 21, 28, and 35 MPa) for acetone by minimizing the objective function.

$$F_{Obj} = \sum_{i=1}^{n} (\eta_i^{\exp} - \eta_i^{cal})^2 \qquad \text{(Eq.5.24)}$$

The parameters are found to be, l = 0.156 $\overset{0}{A}$; E_0 = 58,623 J/mol; and B = 0.02165. For methane Allal et. al. (Allal et. al., 2001) has reported l = 0.590 $\overset{0}{A}$ and B = 0.009 which are of the same order of magnitude. Using the parameters for acetone, we recalculated the viscosities and compared with the experimental data. These are shown in Figure 5.18. The correlation is found to work relatively well at high temperatures. No significant pressure dependence is indicated by the model, which is also the case with experimental data.

A different type of analysis was conducted to test the reliability and predictive ability of the model. Here, parameters, l, E_0, and B were determined using the viscosity data from one temperature and then the viscosities were predicted for other temperatures. The results are shown in Figures 5.19 and 5.20 for correlations based on parameters evaluated using

viscosity data at 398 and 373 K, respectively. As shown in these figures, this model provides reasonable predictions at high pressures, but fails to predict the low temperature data.

Figure 5.21 shows the variations of the parameters with pressure. The model predicts an initial reduction in parameter l which then remains unchanged with further increase in pressure. E_0 term however increases with pressure, which suggests that energy barrier for molecules to diffuse to new vacant sites becomes greater with increasing pressures. This appears reasonable since with increasing pressure, the system becomes compressed and the generation of vacant sites would then require greater energy.

5.4 Summary and conclusions

In the chapter, we have presented density and viscosity data for acetone, carbon dioxide, and acetone + carbon dioxide mixtures containing 10, 25, 50, and 75 wt % carbon dioxide were determined at 323, 348, 373, and 398 K and at pressures up to 35 MPa. The densities of carbon dioxide and acetone +carbon dioxide mixtures were found to show crossovers at around 18 MPa for mixtures with CO_2 content less than 50 wt % and at around 23 MPa for mixtures with CO_2 content greater than 50 wt % at 323 K, which shift to higher pressures with temperature. Acetone displayed higher viscosities than the mixtures. At 323 K, the mixtures were found to show negative excess volumes at all compositions for pressures lower than 28 MPa. The excess volumes become less negative with increasing pressure and above 28 MPa are positive for high carbon dioxide content, and at pressures above 55 MPa become positive for all compositions. Assessments of several mixing rules for viscosity show

that logarithmic equations work well at low temperatures, while simple linear combinations of viscosity or kinematic viscosity work better at higher temperatures. Viscosity of the mixtures could be correlated with density; however there were no direct correlations between excess viscosity and excess volume. Analysis of the excess Gibbs free energy for the flow suggests strong chemical interactions. Modified free-volume models suggest that energy required for molecules to diffuse into the new vacant sites increases with pressure.

Acknowledgements: This chapter is in part based on the publication "*Liu, K., and Kiran, E. (2007). Viscosity, density and excess volume of acetone + carbon dioxide mixtures at high pressures. Industrial & Engineering Chemistry Research, 46, 5453-5462.*". The Industrial & Engineering Chemistry Research is a publication of the American Chemical Society, and the reproduction here is with permission of the American Chemical Society.

Table 5.1 Density (ρ), viscosity (η), excess volume (V^E), excess viscosity ($\Delta\eta$), excess Gibbs free energy ($G_V{}^E$) of viscous flow, and Grunberg-Nissan interaction parameter (d_{12}) of acetone + carbon dioxide mixtures. (Mixture compositions are based on mass)

Acetone				**Acetone/CO_2 = 90/10**							
T (K)	P (MPa)	ρ (g/cm^3)	η (mPa·s)	T (K)	P (MPa)	ρ (g/cm^3)	η (mPa·s)	V^E (cm^3/mol)	$\Delta\eta$ (mPa·s)	$G_V{}^E$ (kJ/mol)	d_{12} (-)
323	7.5	0.7584	0.290	325	7.9	0.7641	0.281				
323	14.3	0.7631	0.367	325	14.3	0.7736	0.289	-1.297	-0.037	-0.027	0.041
323	21.4	0.7704	0.362	325	21.2	0.7832	0.294	-0.850	-0.031	-0.021	-0.012
323	27.8	0.7773	0.377	325	28.2	0.7902	0.307	-0.357	-0.032	-0.024	-0.105
323	35.0	0.7838	0.383	325	34.7	0.7983	0.311	-0.236	-0.035	-0.056	-0.238
348	8.1	0.7370	0.244	348	7.4	0.7373	0.236				
348	14.4	0.7462	0.253	349	14.7	0.7503	0.243				
348	21.4	0.7546	0.255	349	21.4	0.7619	0.247	-0.436	0.018	0.512	1.571
348	28.3	0.7623	0.262	349	28.3	0.7702	0.254	-0.381	0.018	0.446	1.359
348	35.1	0.7697	0.264	349	34.8	0.7793	0.260				
373	8.3	0.7177	0.200	374	7.1	0.7192	0.191				
373	14.7	0.7285	0.203	374	14.3	0.7305	0.201				
373	21.3	0.7384	0.215	374	21.3	0.7401	0.206				
373	28.6	0.7474	0.214	374	28.3	0.7488	0.210	-0.832	0.018	0.529	1.588
373	35.3	0.7555	0.232	374	35.2	0.7599	0.215	-0.520	0.006	0.307	0.905
398	8.2	0.6919	0.169	399	7.0	0.6999	0.160				
398	13.5	0.7058	0.162	399	14.5	0.7070	0.164				
398	20.5	0.7174	0.182	399	21.3	0.7183	0.169				
398	27.9	0.7282	0.184	399	27.9	0.7305	0.175				
398	33.7	0.7374	0.205	399	34.9	0.7389	0.182				

Acetone/CO_2 = 75/25								Acetone/CO_2 = 50/50							
T (K)	P (MPa)	ρ (g/cm^3)	η (mPa·s)	V^E (cm^3/mol)	$\Delta\eta$ (mPa·s)	G_V^E (kJ/mol)	d_{12} (-)	T (K)	P (MPa)	ρ (g/cm^3)	η (mPa·s)	V^E (cm^3/mol)	$\Delta\eta$ (mPa·s)	G_V^E (kJ/mol)	d_{12} (-)
325	7.8	0.7708	0.225					325	7.1	0.7885	0.137				
324	15.0	0.7850	0.233	-2.683	0.016	0.244	0.576	325	14.2	0.8134	0.145	-5.499	-0.045	0.154	0.554
326	21.0	0.7977	0.241	-1.579	0.016	0.207	0.417	325	21.2	0.8303	0.152	-3.322	-0.045	0.009	0.180
324	28.0	0.8051	0.252	-0.430	0.014	0.180	0.271	325	28.1	0.8389	0.161	-1.250	-0.050	-0.015	-0.015
323	34.9	0.8145	0.259	-0.049	0.015	0.162	0.199	325	34.9	0.8511	0.168	-0.507	-0.051	-0.033	-0.108
349	7.4	0.7378	0.185					348	7.3	0.7401	0.113				
349	14.0	0.7584	0.193					348	14.2	0.7705	0.120				
349	21.2	0.7721	0.199	-0.961	0.013	0.723	1.182	348	21.2	0.7903	0.127	-1.918	-0.012	0.595	0.913
349	28.2	0.7815	0.203	-0.845	0.008	0.534	0.866	348	28.1	0.8011	0.133	-1.672	-0.016	0.342	0.537
349	35.0	0.7934	0.211					348	35.1	0.8175	0.141				
373	7.5	0.7203	0.164												
374	14.3	0.7321	0.171					373	15.7	0.7353	0.111				
373	21.0	0.7415	0.178					373	21.3	0.7502	0.119				
373	27.9	0.7532	0.185	-2.213	0.026	0.934	1.532	374	28.3	0.7685	0.125	-5.016	0.007	0.824	1.368
373	34.7	0.7668	0.191	-1.271	0.024	0.683	1.078	374	35.2	0.7840	0.132	-2.942	-0.002	0.557	0.881
398	16.5	0.7083	0.141												
398	21.3	0.7192	0.147					398	22.8	0.7216	0.083				
398	28.0	0.7354	0.156					398	27.9	0.7378	0.090				
398	34.5	0.7409	0.162					398	34.4	0.7430	0.096				

Acetone/CO_2 = 25/75								Carbon Dioxide			
T (K)	P (MPa)	ρ (g/cm^3)	η (mPa·s)	V^E (cm^3/mol)	$\Delta\eta$ (mPa·s)	G_V^E (kJ/mol)	d_{12} (-)	T (K)	P (MPa)	ρ (g/cm^3)	η (mPa·s)
326	7.40	0.6653	0.105								
326	14.54	0.7949	0.111	-4.481	-0.008	0.621	1.864	320	13.8	0.7305	0.057
326	21.01	0.8339	0.117	-2.714	-0.014	0.303	0.940	320	20.0	0.8035	0.073
326	27.87	0.8435	0.125	0.153	-0.019	0.273	0.531	320	27.2	0.8705	0.085
326	35.17	0.8603	0.131	1.062	-0.021	0.223	0.292	320	34.1	0.9127	0.095
350	14.99	0.6995	0.093								
350	21.53	0.7773	0.098	-0.300	0.006	0.986	2.100	355	23.9	0.7793	0.051
350	28.24	0.7923	0.105	-0.210	0.002	0.661	1.387	355	31.5	0.7983	0.063
350	34.88	0.8125	0.112								
374	27.78	0.7185	0.095	-1.939	0.015	1.191	2.557	369	28.6	0.6823	0.047
374	34.99	0.7512	0.104	-0.395	0.011	0.918	1.848	369	34.4	0.7430	0.059

Table 5.2 Parameters for viscosity correlation with pressure (Mixture compositions are based on mass) (Equation 5.2)

System	Activation volume, $V^{\neq}$ (cm^3/mol)				A (× 10^4) (mPa•s)				Correlation coefficient R				AAD[a] (× 10^3) (mPa•s)			
	Temperature (K)				Temperature (K)				Temperature (K)				Temperature (K)			
	323	*348*	*373*	*398*	*323*	*348*	*373*	*398*	*323*	*348*	*373*	*398*	*323*	*348*	*373*	*398*
Acetone	5	9	16	26	2.89	2.41	1.92	1.52	0.82	0.84	0.95	0.72	6	4	1	3
Acetone/CO_2 = 90/10	11	10	12	16	2.72	2.29	1.88	1.54	0.97	0.99	0.96	0.99	2	1	1	1
Acetone/CO_2 = 75/25	15	13	17	26	2.16	1.80	1.58	1.23	0.99	0.98	0.99	0.99	1	1	1	1
Acetone/CO_2 = 50/50	20	23	27	41	1.30	1.07	0.98	0.63	0.99	0.99	0.98	0.98	0	0	1	1
Acetone/CO_2 = 25/75	22	28	39	-	0.99	0.81	0.67	-	0.99	0.99	0.99	-	0	0	0	-
	Temperature (K)				Temperature (K)											
	320	*355*	*370*		*320*	*355*	*370*									
CO_2	7	9	12		0.42	0.25	0.40	-	0.95	0.99	0.99	-	3	2	0	-

[a] Average absolute deviation = $\left|X_O - X_P\right| / N$, where X_O is the value observed, X_P is the value predicted from the model, and *N* is the number of the data points.

Table 5.3 Parameters for viscosity correlation with temperature (Mixture compositions are based on mass) (Equation 5.3)

System	Activation energies, $E^{\neq}$ (kJ/mol)					B (× 10^5) (mPa•s)					Correlation coefficient R					AAD (× 10^3) (mPa•s)				
	Pressure (MPa)					Pressure (MPa)					Pressure (MPa)					Pressure (MPa)				
	7	*14*	*21*	*28*	*35*	*7*	*14*	*21*	*28*	*35*	*7*	*14*	*21*	*28*	*35*	*7*	*14*	*21*	*28*	*35*
Acetone	8	10	8	8	6	1.67	1.24	2.49	2.04	3.72	0.99	0.98	0.99	0.99	0.99	3	7	5	4	0
Acetone/CO_2 = 90/10	8	8	8	8	8	1.37	1.37	1.51	1.51	1.85	0.99	0.99	0.99	0.99	0.99	2	4	4	2	2
Acetone/CO_2 = 75/25	7	7	7	7	6	2.04	1.67	1.85	2.25	2.25	0.99	0.99	0.99	0.99	0.99	2	3	3	4	3
Acetone/CO_2 = 50/50	8	6	8	8	8	0.68	0.71	0.75	0.92	1.01	0.99	0.95	0.90	0.90	0.90	0	3	6	6	6
Acetone/CO_2 = 25/75	-	7	7	6	5	-	0.83	0.92	1.51	2.25	-	0.99	0.99	0.99	0.97	-	0	0	1	2

Table 5.4 Parameters for viscosity correlation with density (Mixture compositions are based on mass) (Equation 5.4)

System	Doolittle equation parameters			Correlation coefficient R	AAD
	C (mPa•s)	D (-)	V_0 (cm^3/g)		($\times 10^2$) (mPa•s)
Acetone	1.20E-02	0.80	0.98	0.91	0.7
Acetone/CO_2 = 90/10	1.00E-03	2.67	0.67	0.94	1.5
Acetone/CO_2 = 75/25	1.00E-03	2.67	0.64	0.93	1.2
Acetone/CO_2 = 50/50	1.00E-03	2.67	0.57	0.93	0.8
Acetone/CO_2 = 25/75	1.00E-03	2.67	0.54	0.93	1.3
CO_2	1.00E-03	2.67	0.45	0.95	0.4

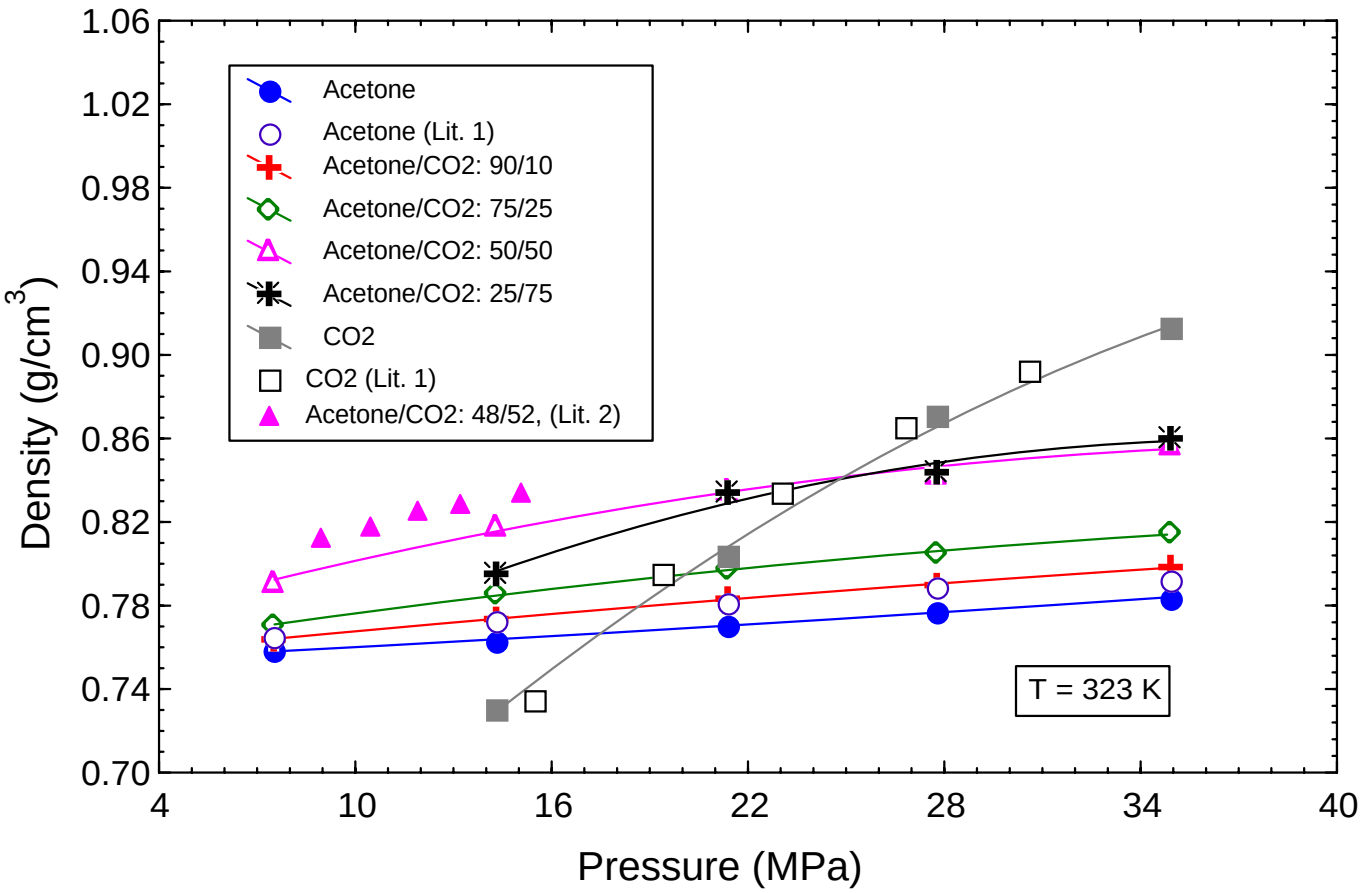

Figure 5.1 Variation of density with pressure at the nominal temperature of 323 K for acetone, carbon dioxide, and acetone + carbon dioxide mixtures containing 10, 25, 50, and 75 wt % carbon dioxide. (See Table 5.1 for exact temperature for each mixture). Lit. 1: Pöhler and Kiran, 1997a; Lit 2: Chen et. al., 2003.

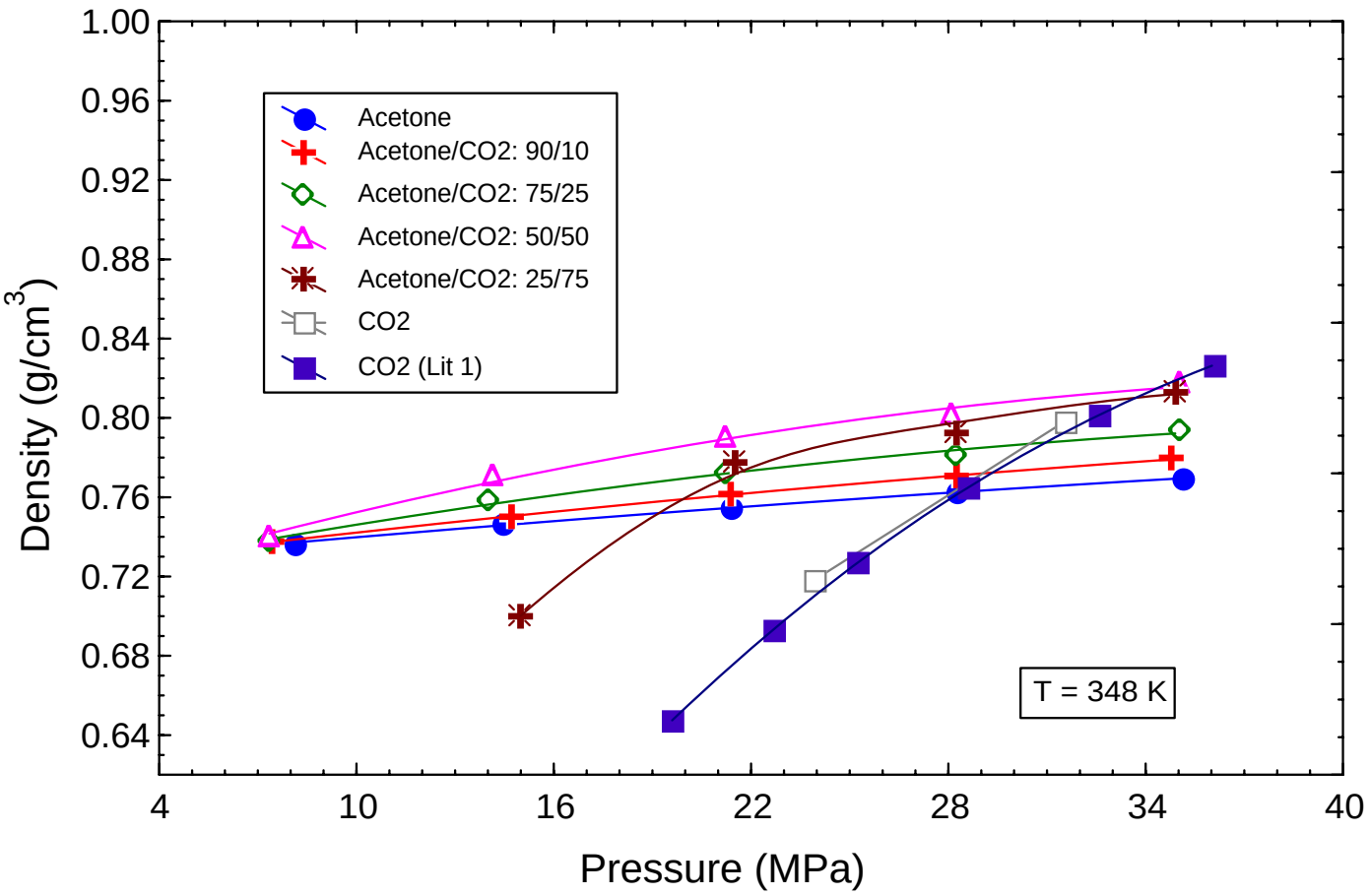

Figure 5.2 Variation of density with pressure at the nominal temperature of 348 K for acetone, carbon dioxide, and acetone + carbon dioxide mixtures containing 10, 25, 50, and 75 wt % carbon dioxide. (See Table 5.1 for exact temperature for each mixture). Lit. 1. Pholer and Kiran, 1997a.

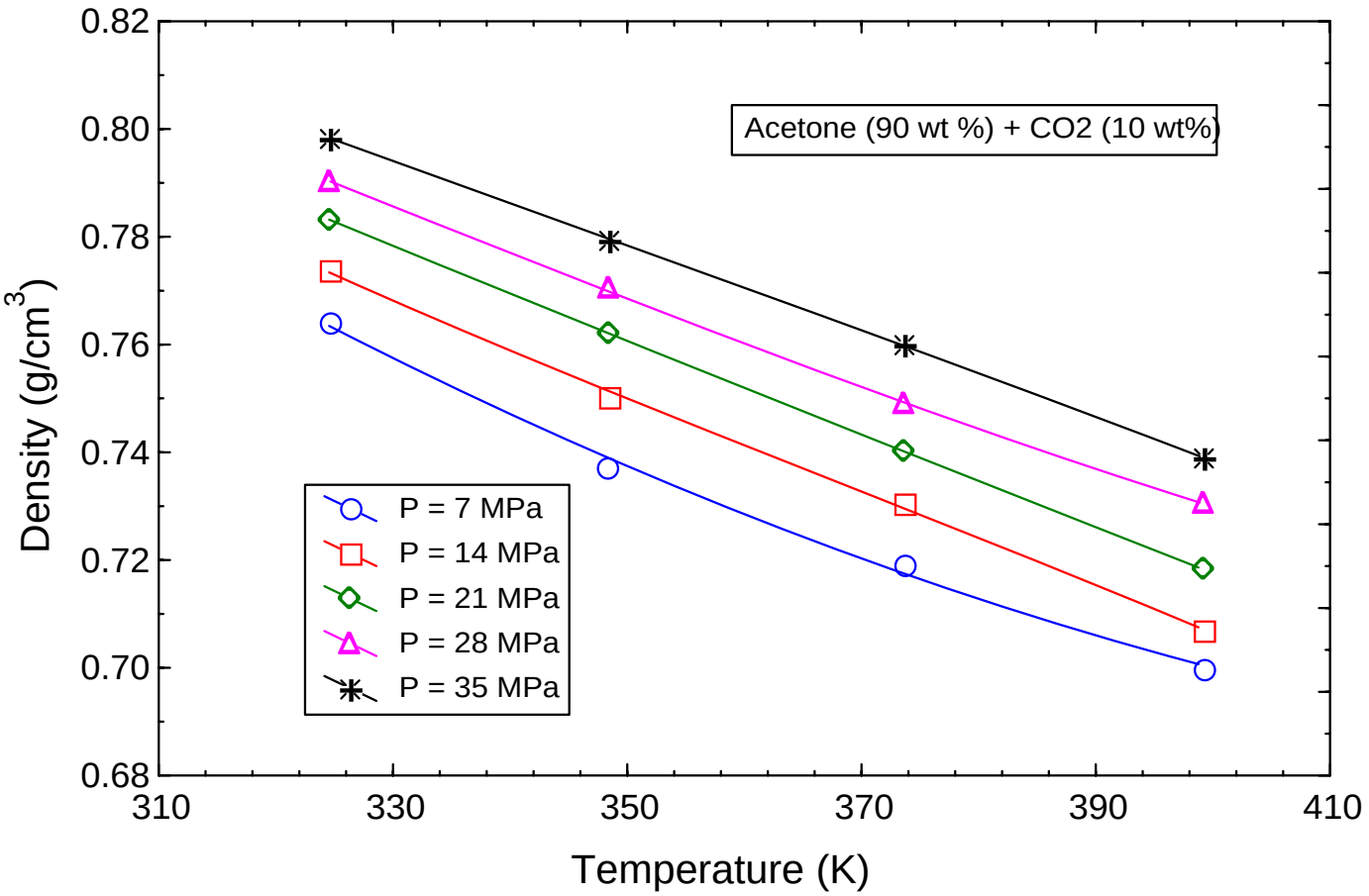

Figure 5.3 Variation of density with temperature for acetone + carbon dioxide mixtures containing 10 wt % carbon dioxide at 7, 14, 21, 28, and 35 MPa.

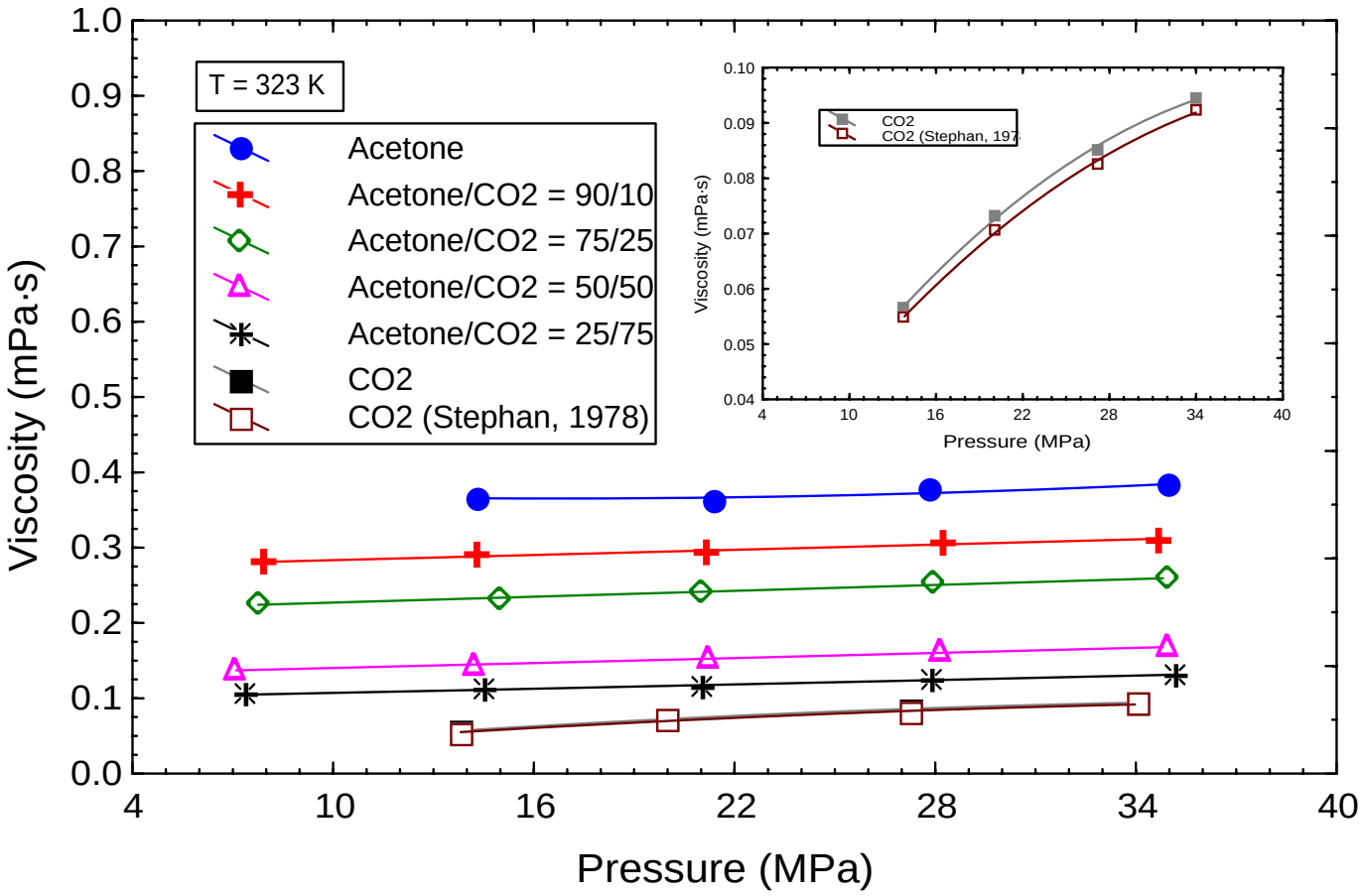

Figure 5.4 Variation of viscosity with pressure at 323 K for acetone, carbon dioxide, and acetone + carbon dioxide mixtures containing 10, 25, 50, and 75 wt % carbon dioxide.

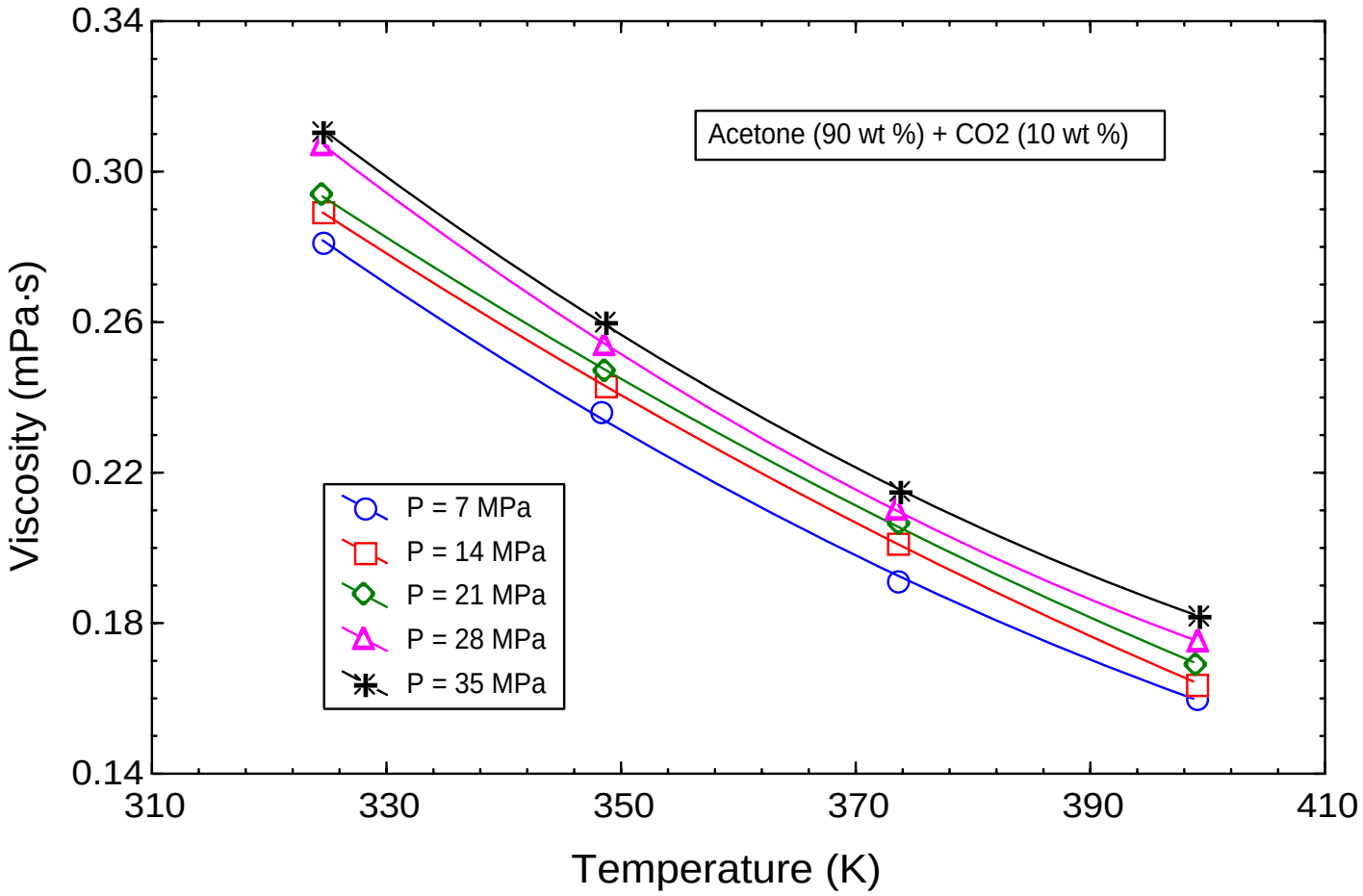

Figure 5.5 Variation of viscosity with temperature for acetone + carbon dioxide mixture containing 10 wt % carbon dioxide at 7, 14, 21, 28, and 35 MPa.

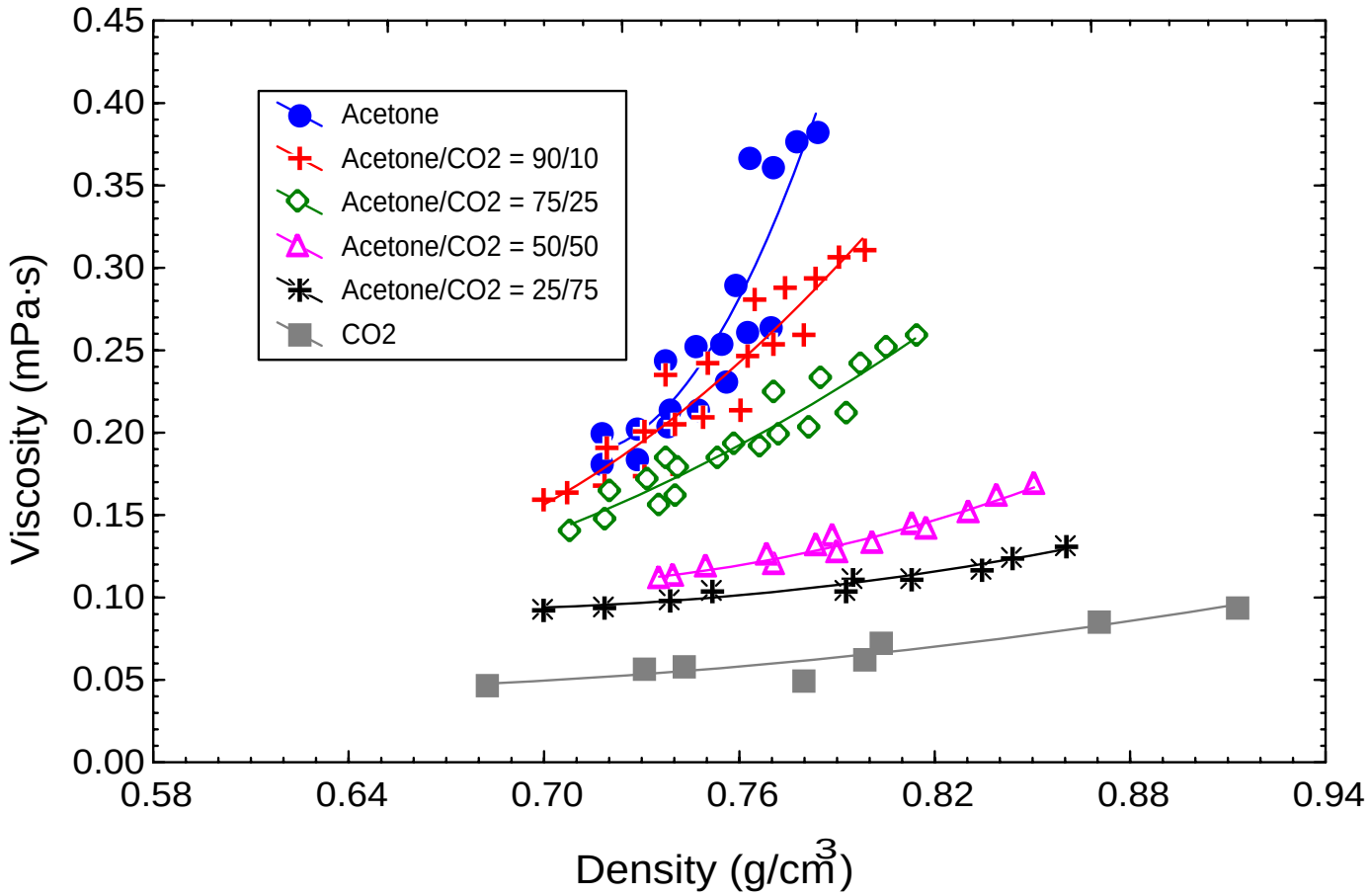

Figure 5.6 Variation of viscosity with density for acetone, carbon dioxide, and acetone + carbon dioxide mixtures containing 10, 25, 50, and 75 wt % carbon dioxide.

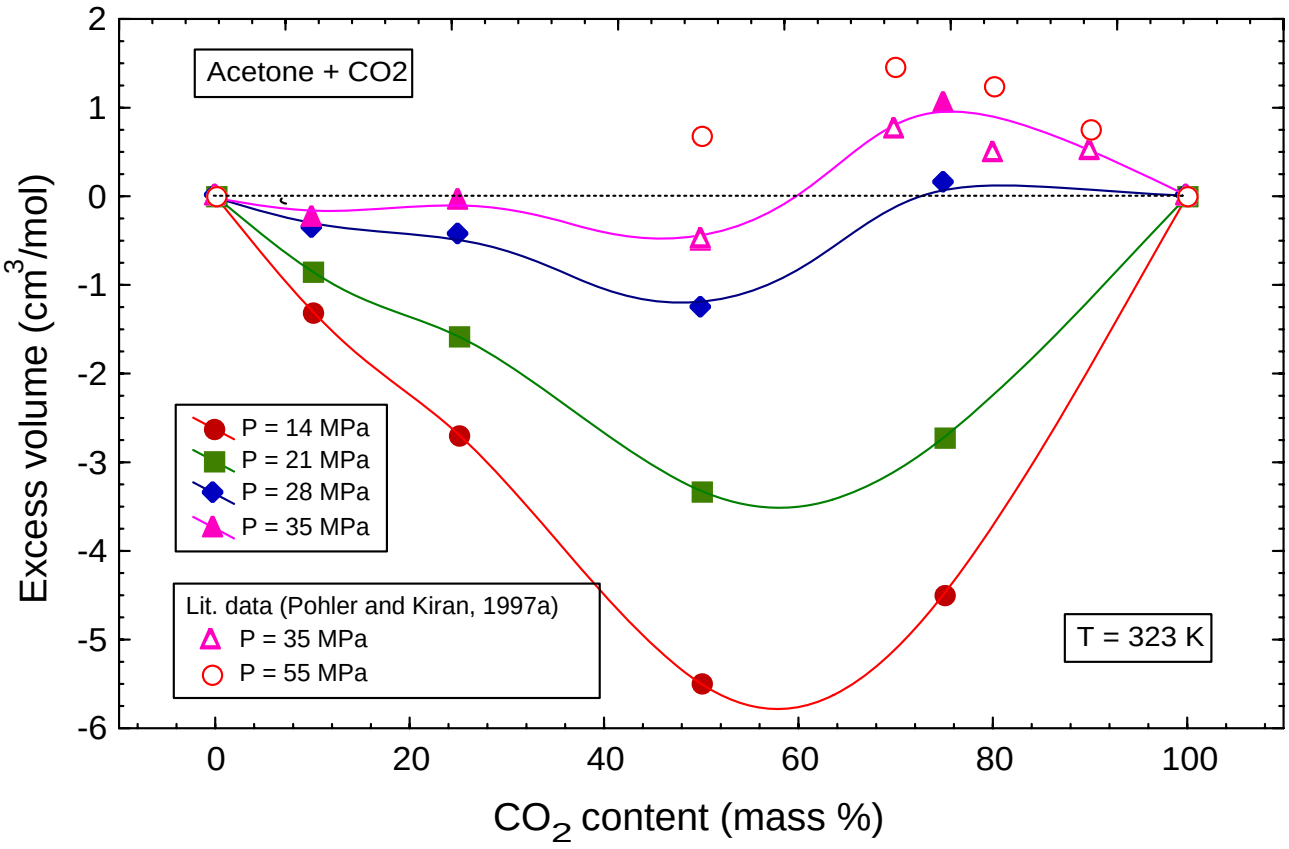

Figure 5.7 Variation of excess volume with carbon dioxide content for acetone + carbon dioxide mixture at 323 K and at 14, 21, 28, and 35 MPa. Excess volumes at 35 and 55 MPa are from literature (Pohler and Kiran, 1997a).

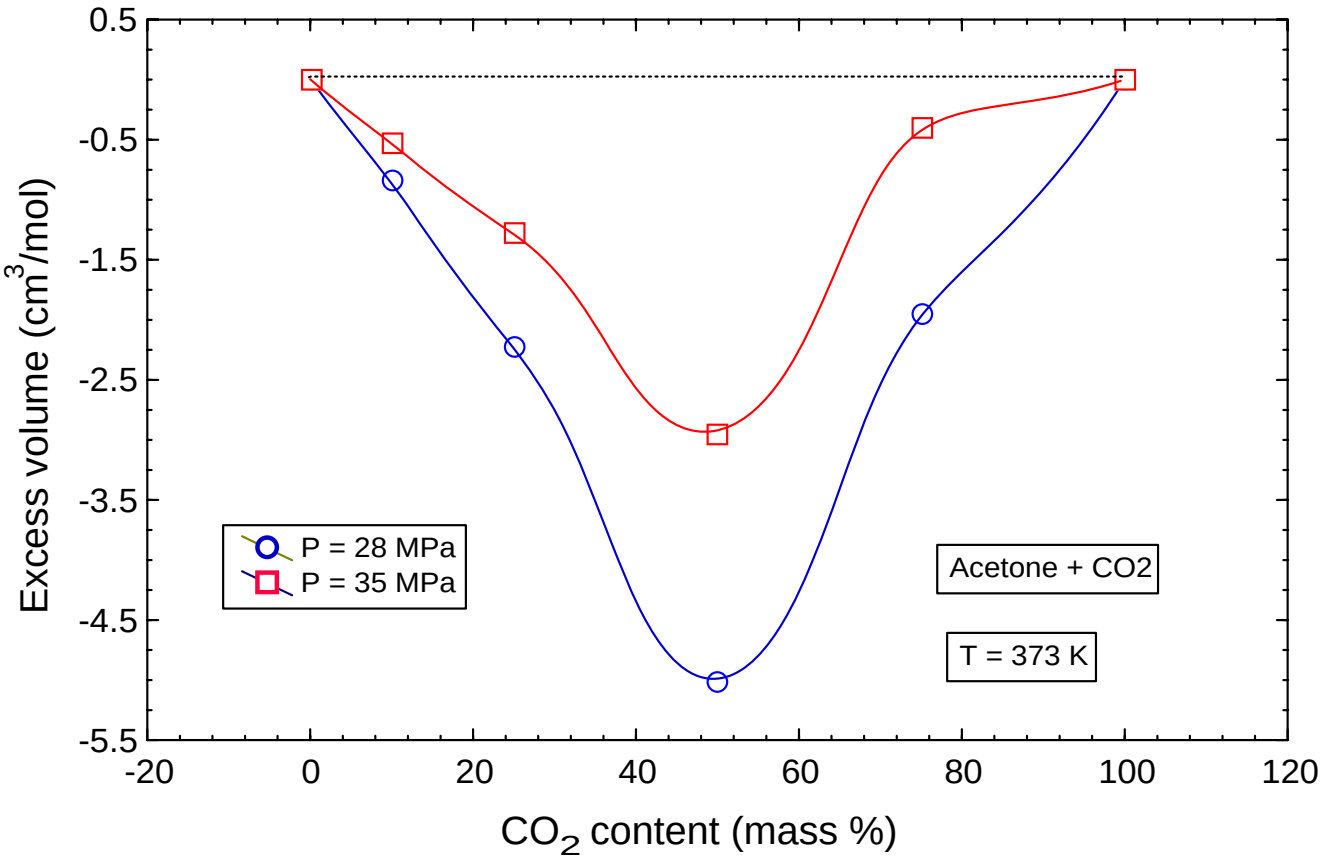

Figure 5.8 Variation of excess volume with carbon dioxide content for acetone + carbon dioxide mixture at 373 K and 28 and 35 MPa.

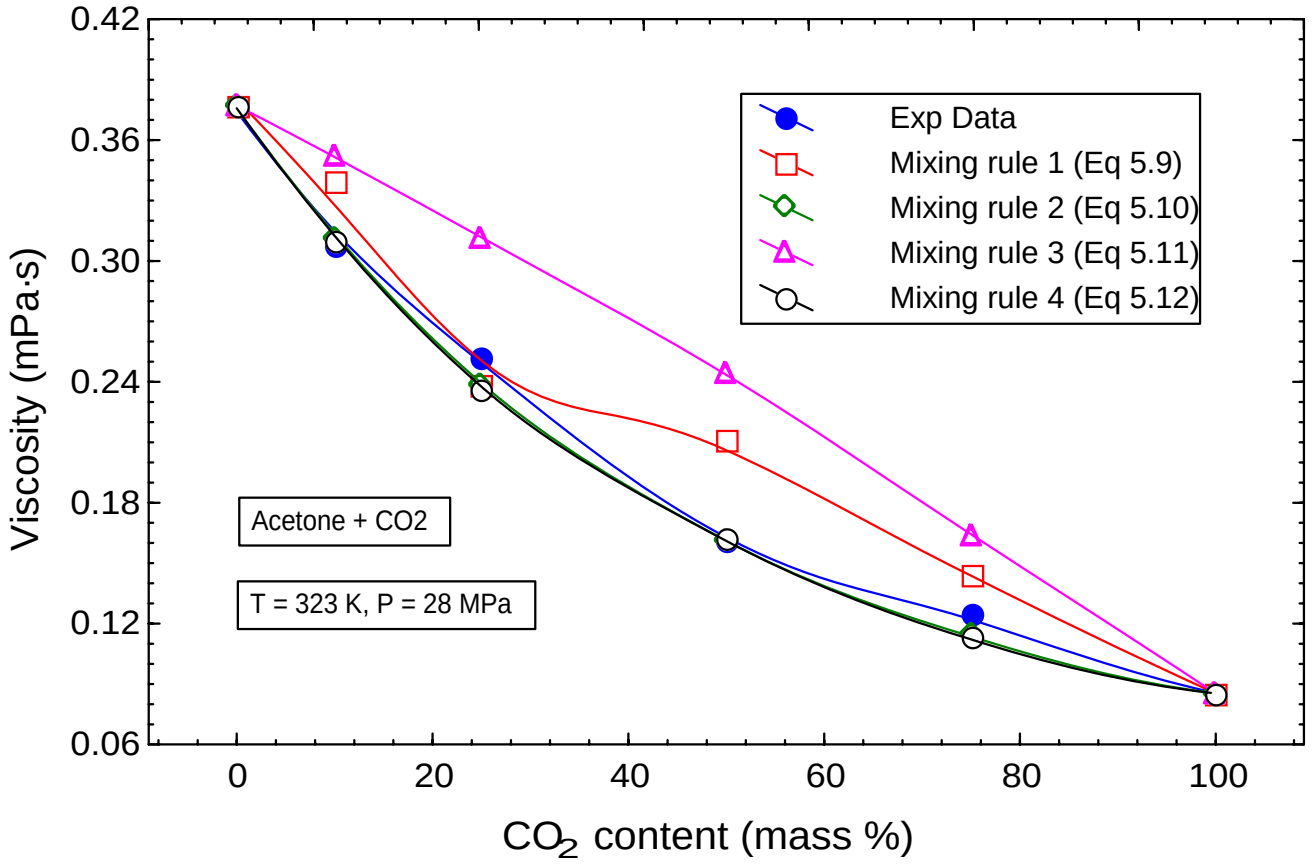

Figure 5.9 Variation of viscosity with carbon dioxide content for acetone + carbon dioxide mixture at 323 K and 28 MPa. The viscosities include the experimental data and data calculated from 4 different mixing rules. See text for the mixing rules.

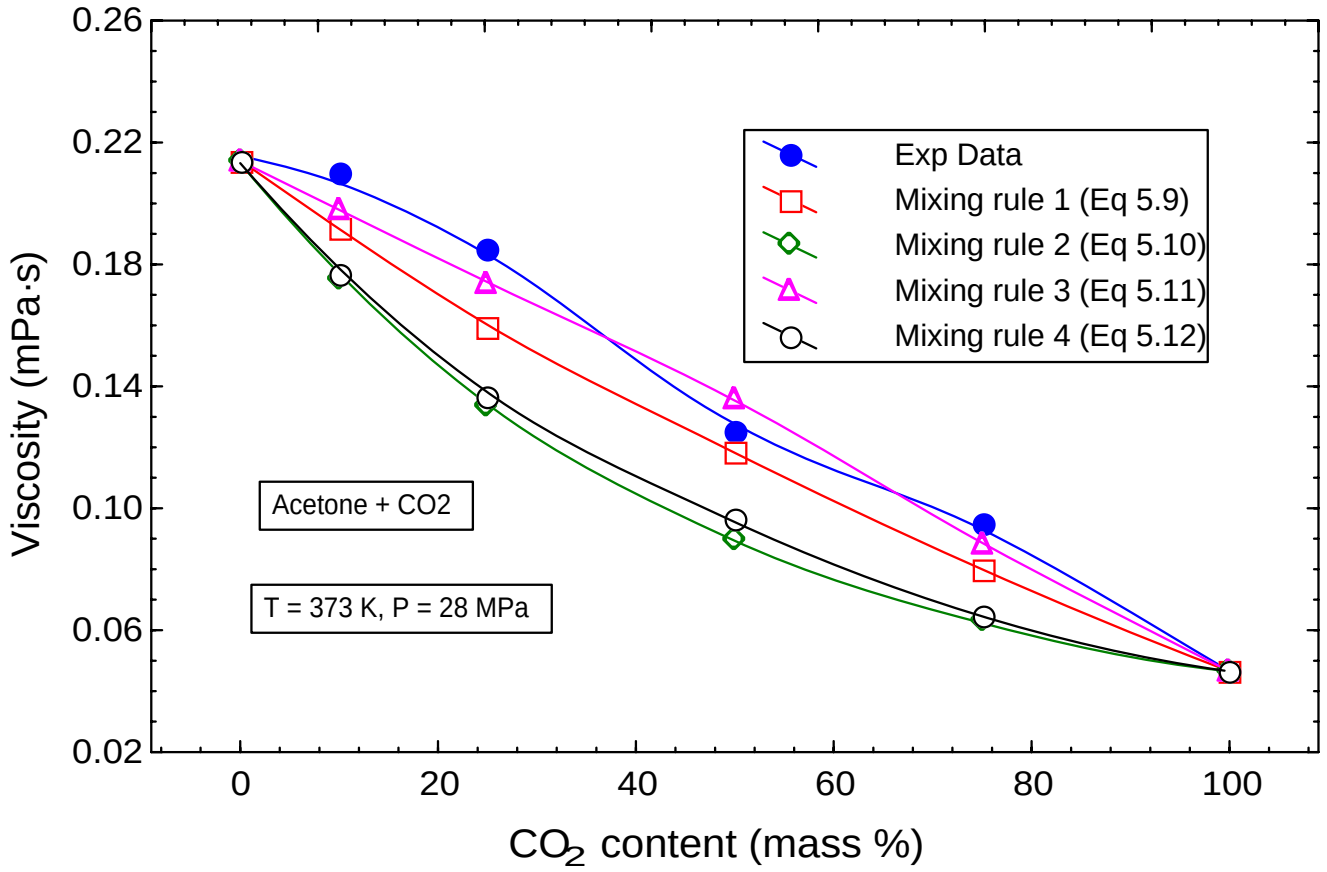

Figure 5.10 Variation of viscosity with carbon dioxide content for acetone + carbon dioxide mixture at 373 K and 28 MPa. The viscosities include the experimental data and data calculated from 4 different mixing rules. See text for the mixing rules.

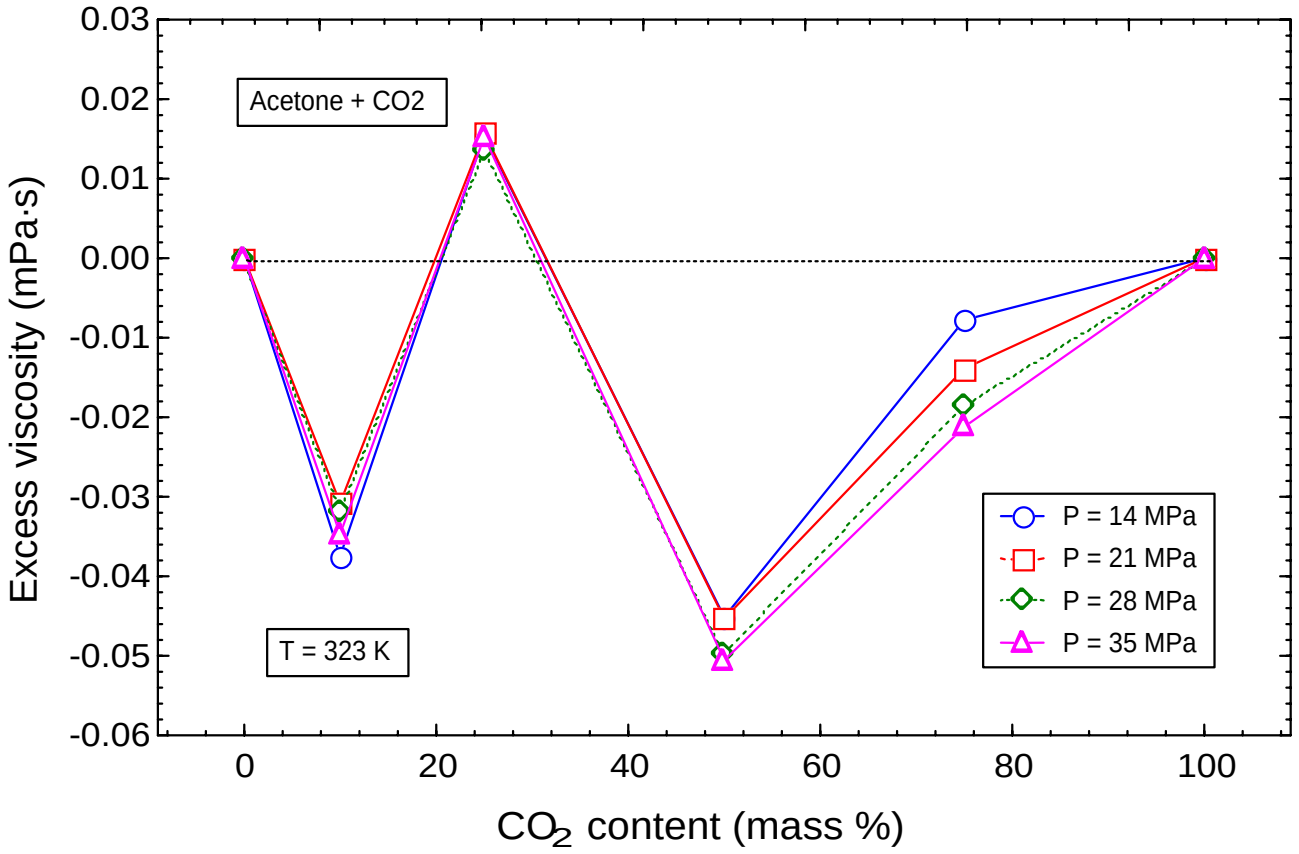

Figure 5.11 Variation of excess viscosity with carbon dioxide content (mass %) for acetone + carbon dioxide mixture at 323 K and at 14, 21, 28, and 35 MPa.

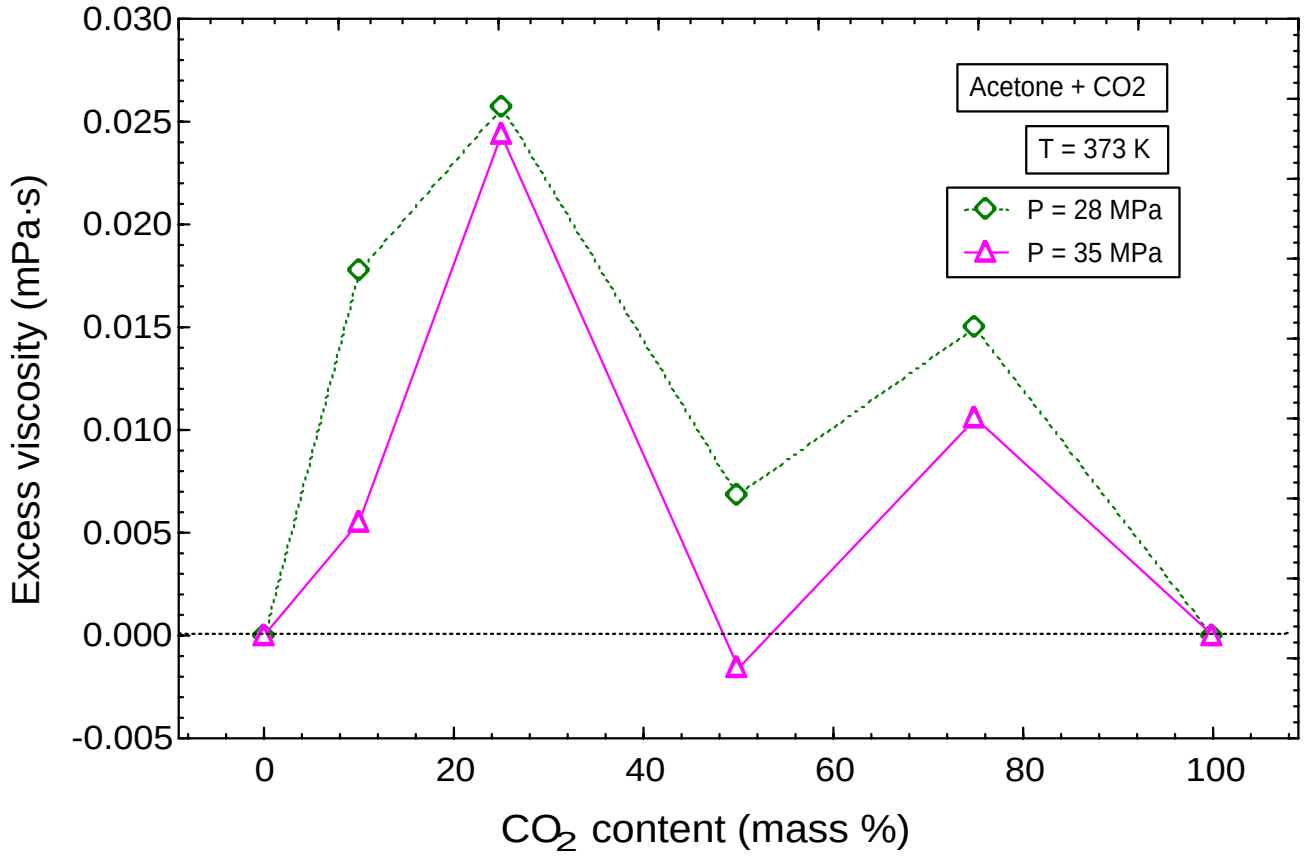

Figure 5.12 Variation of excess viscosity with carbon dioxide content (mass %) for acetone + carbon dioxide mixture at 373 K and at 28 and 35 MPa.

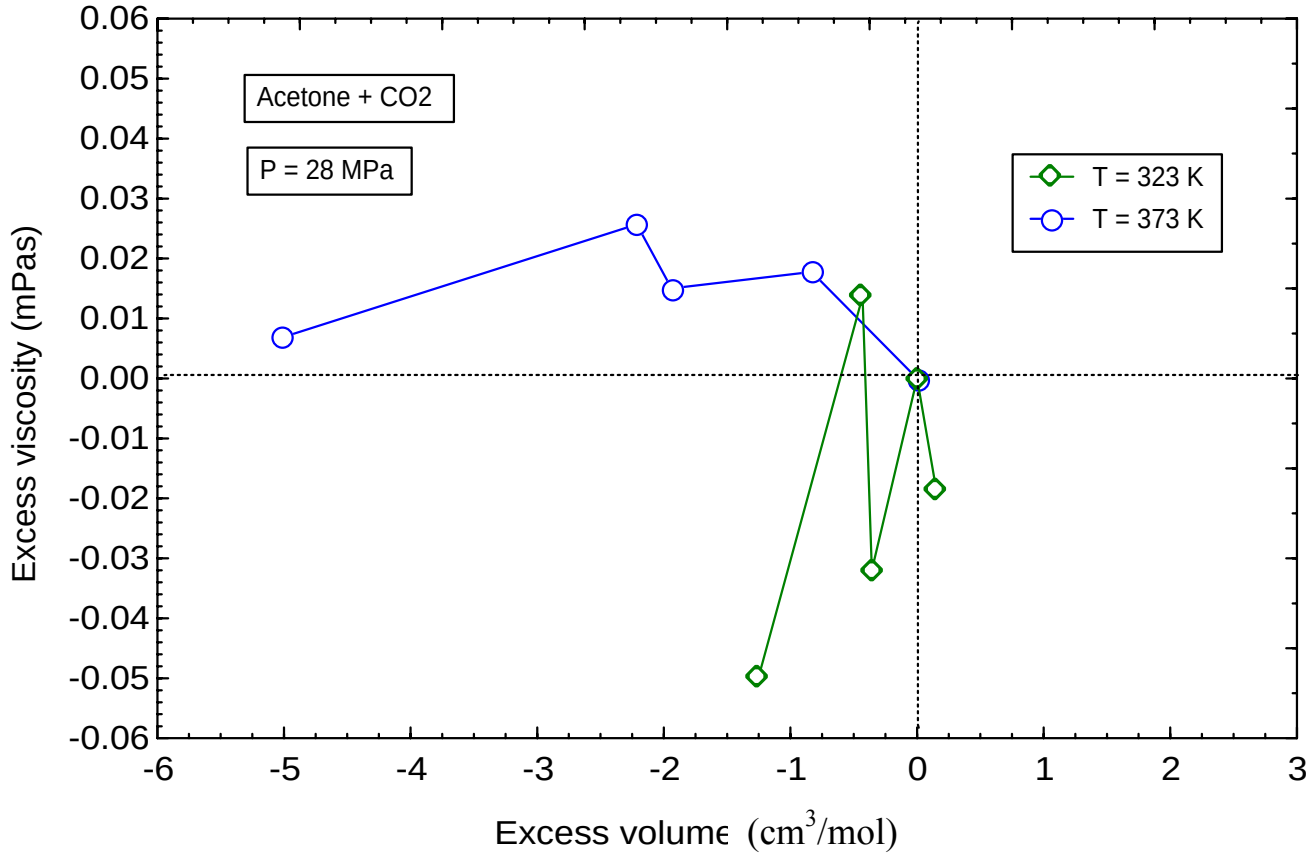

Figure 5.13 Variation of excess viscosity with excess volume for acetone + carbon dioxide mixtures containing 0, 10, 25, 50, 75, and 100 wt % carbon dioxide at 323 K and 373 K at 28 MPa.

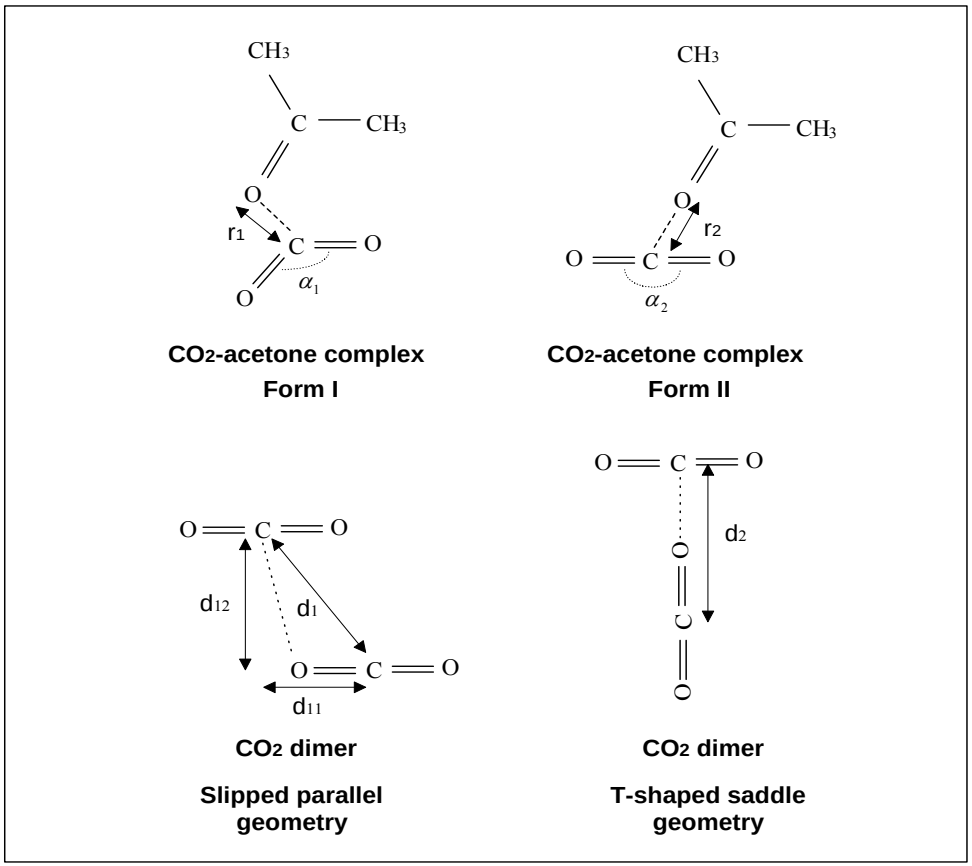

Figure 5.14 *Top*: Electron donor-acceptor complexes between acetone and carbon dioxide (Cabaco et. al., 2005)[35] where $\alpha_1 = 132.8$ °, $r_1 = 2.745$ Å; $\alpha_2 = 180.0$ °, $r_2 = 2.774$ Å. *Bottom*: Dimer structures of carbon dioxide: the slipped parallel arrangement with C- C distance of 3.6 Å ($d_1 = 3.6$ Å, $d_{11} = 1.9$ Å, $d_{12} = 3.1$ Å) and T – shaped arrangement with C – C distance of 4.2 Å. ($d_2 = 4.2$ Å) (Fedchenia and Schröder, 1997)

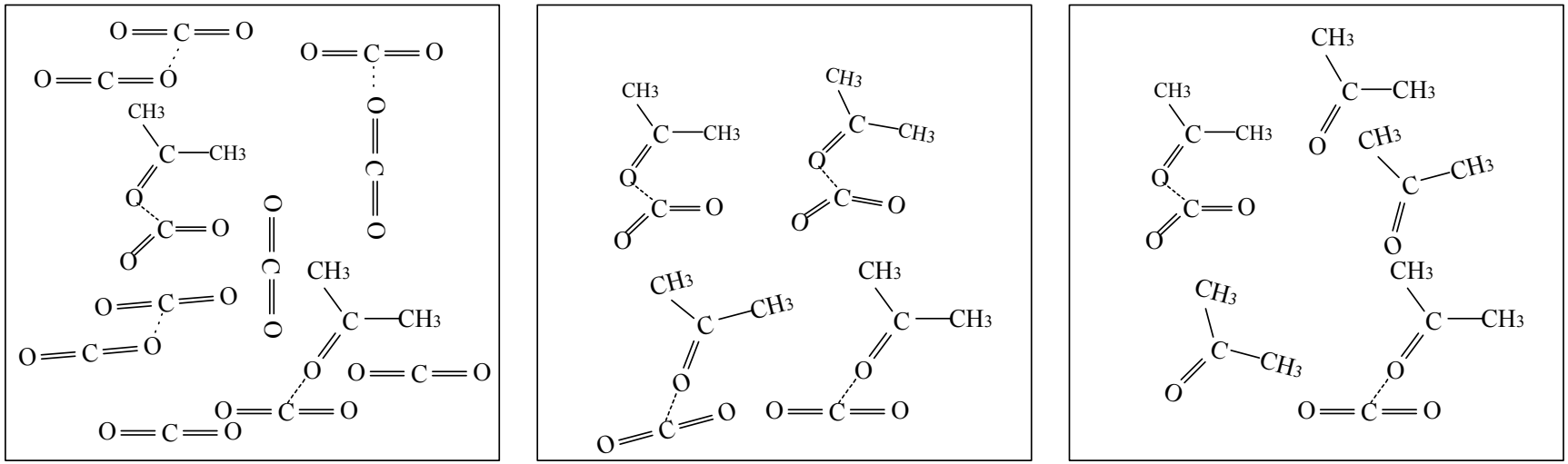

CO_2: Acetone > 1 CO_2:Acetone = 1 CO_2 : Acetone < 1

Figure 5.15 Visualization of compositional variations in carbon dioxide – acetone mixtures. The diagrams consider possibilities for different forms of CO_2 dimers, and CO_2-acetone complexes for different CO_2 :acetone ratios in the mixtures.

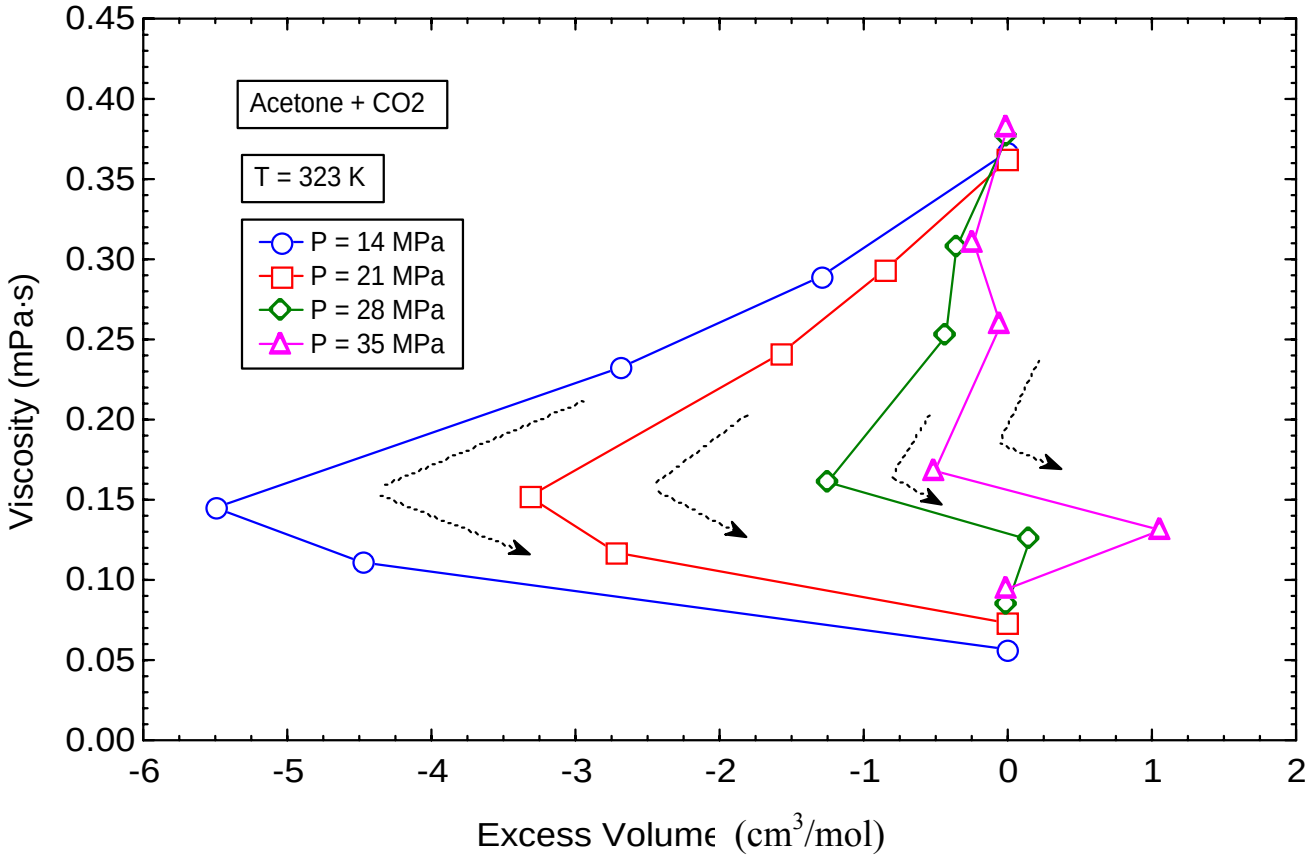

Figure 5.16 Variation of viscosity with excess volume for acetone + carbon dioxide mixture at 323 K and 14, 21, 28, and 35 MPa. On each curve, from top to the bottom, the carbon dioxide contents for every point are 0, 10, 25, 50, 75, and 100 wt %.

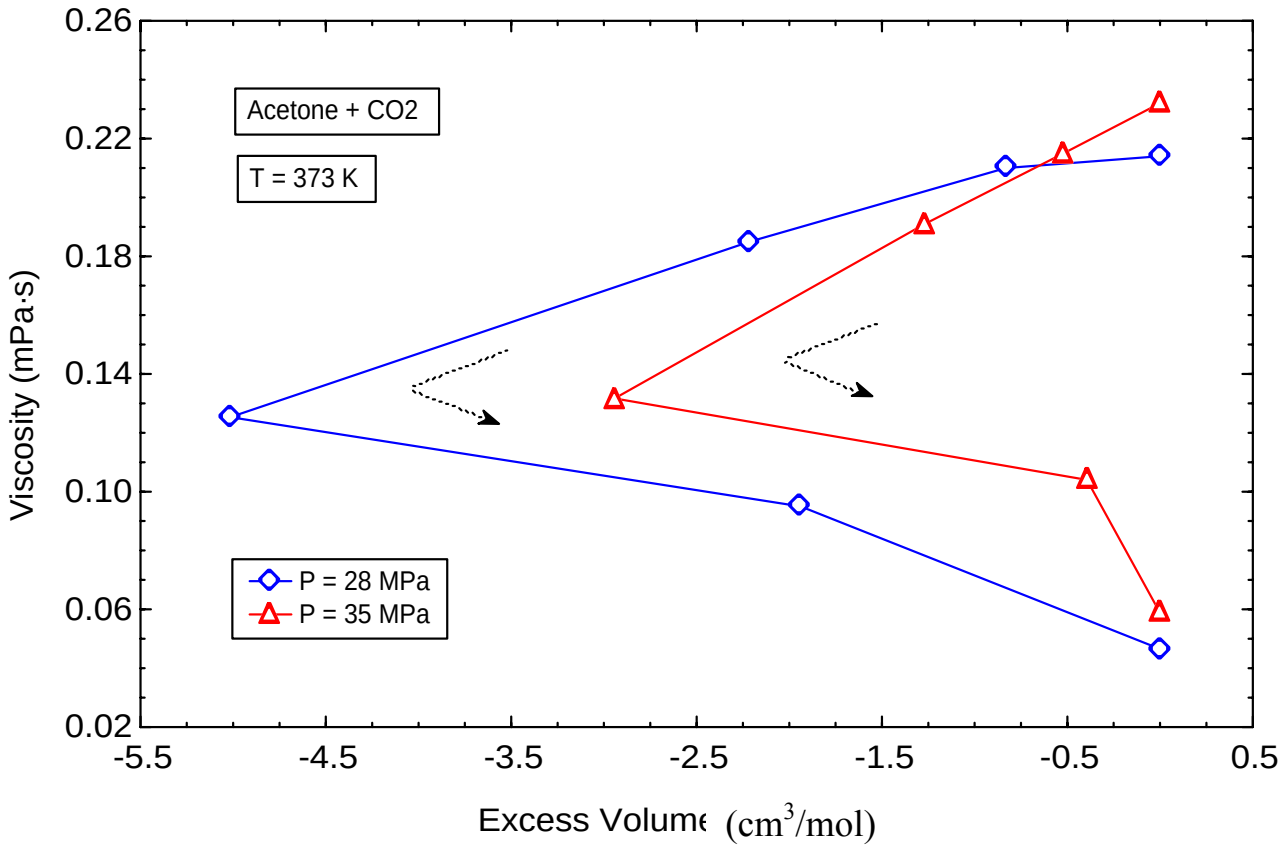

Figure 5.17 Variation of viscosity with excess volume for acetone + carbon dioxide mixture at 373 K and 28 and 35 MPa. On each curve, from top to the bottom, the carbon dioxide contents for every point are 0, 10, 25, 50, 75, and 100 wt %.

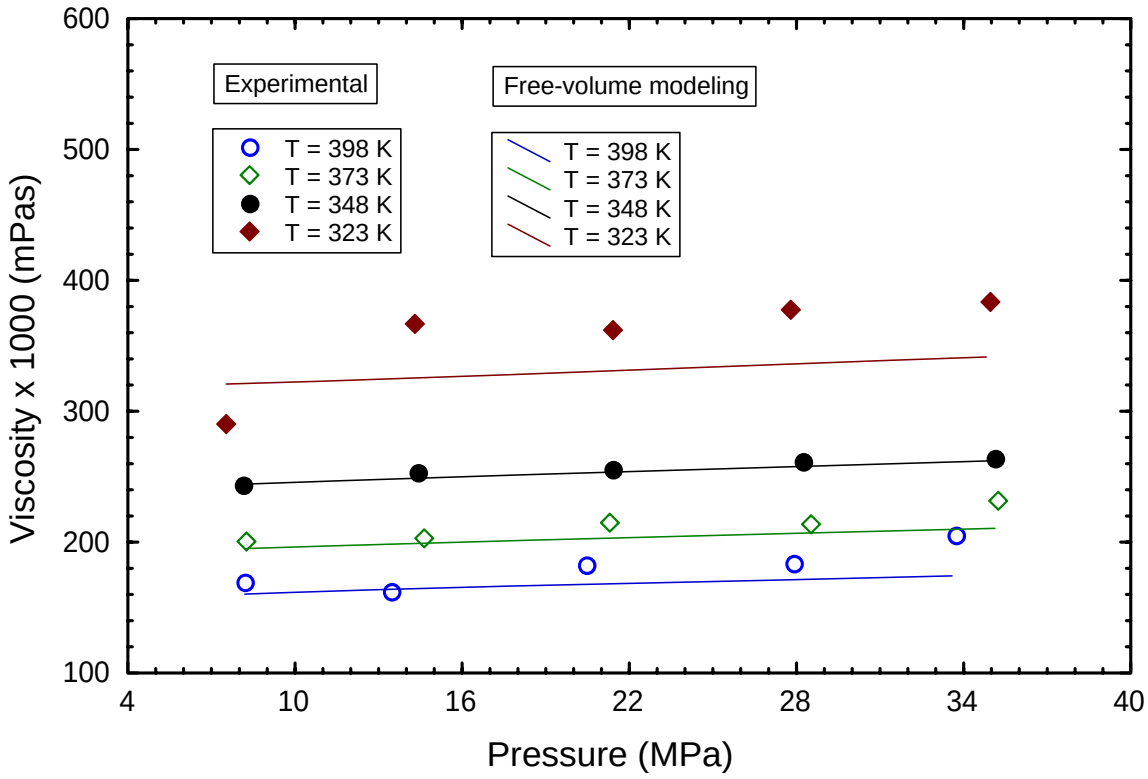

Figure 5.18 Correlation results for acetone using all the experimental data.

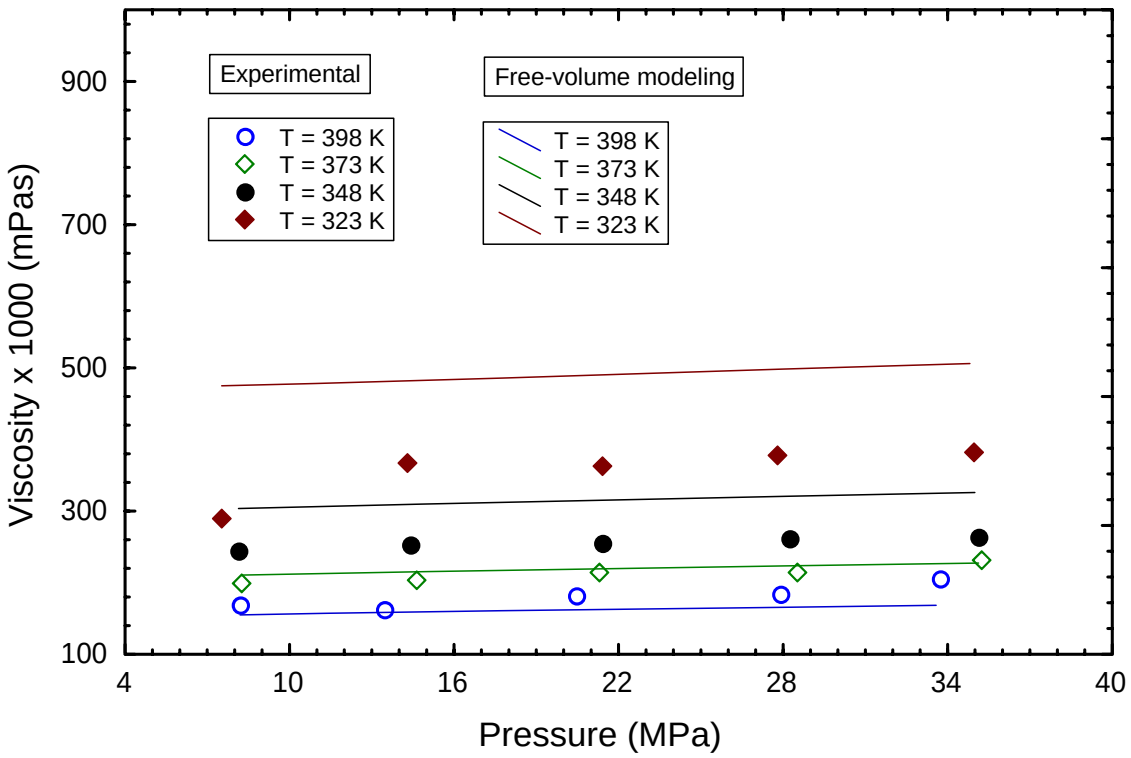

Figure 5.19 Correlation results. In this correlation, the parameters that were determined from data at 398 K were used to predict the viscosity at T = 373, 348, and 323 K.

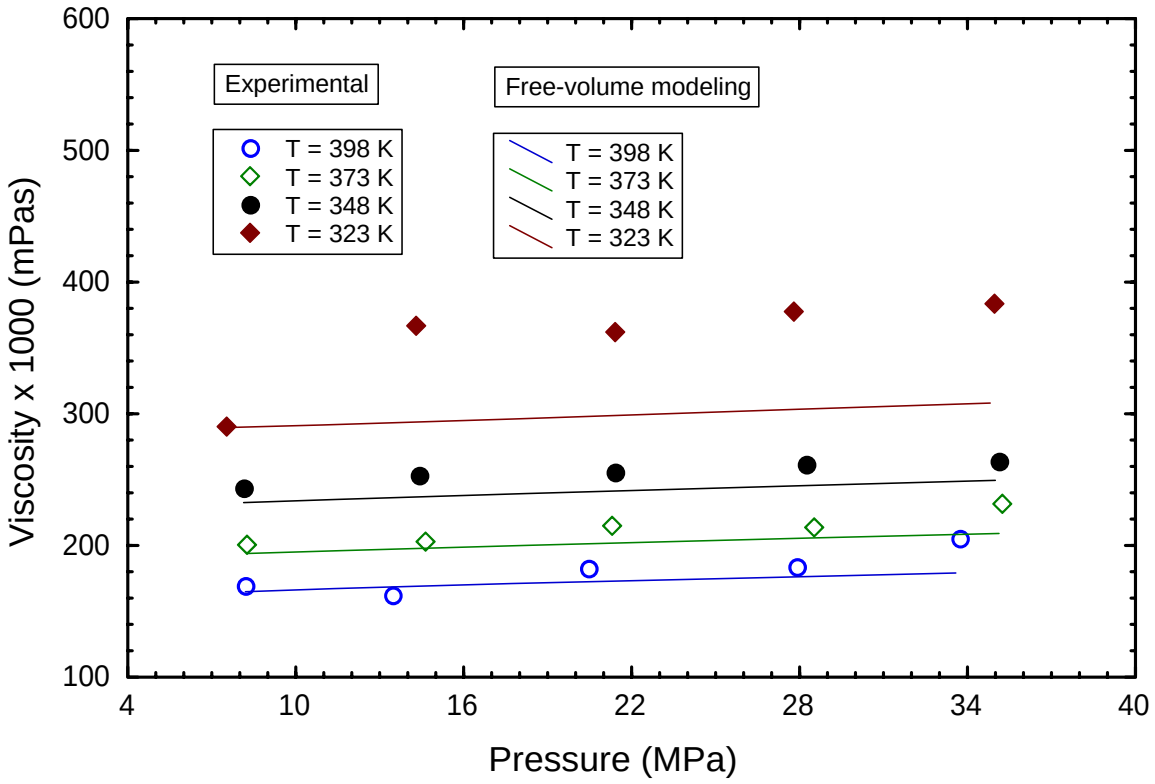

Figure 5.20 Correlation results. In this correlation, the parameters that were determined from data at 373 K were used to predict the viscosity at T = 398, 348, and 323 K.

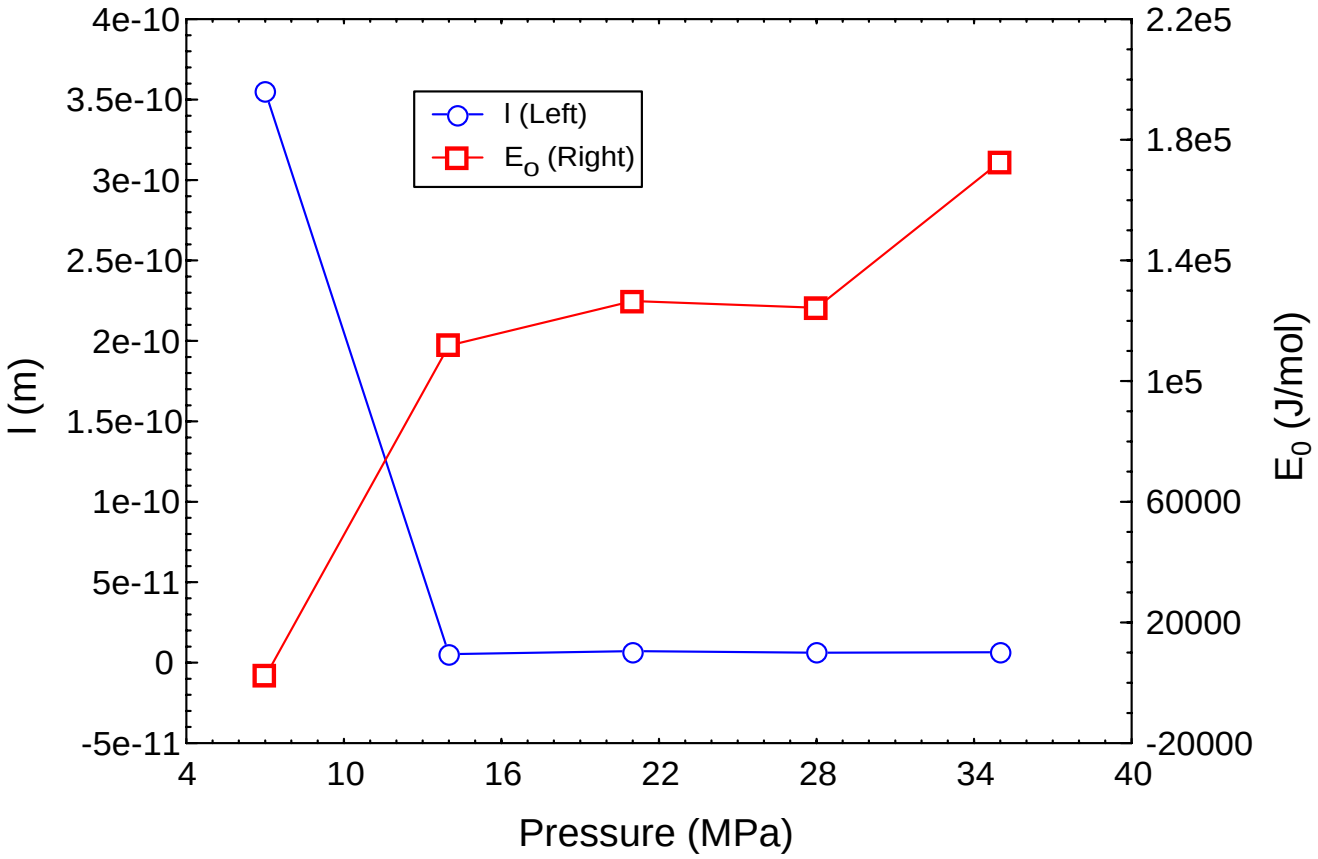

Figure 5.21 Variations of model parameters, l and E_0, with pressure. The parameters were determined at fixed pressure.